EARTHQUAKE ENGINEERING AND STRUCTURAL DYNAMICS, VOL. 25, 1433–1467 (1996)

DUAL-LEVEL SEISMIC DESIGN: A RELIABILITY-BASED METHODOLOGY

KEVIN R. COLLINS*

Department of Civil and Environmental Engineering, 2374 G.G. Brown Building, 2350 Hayward, University of Michigan, Ann Arbor, MI 48109-2125, U.S.A.

AND

YI-KWEI WEN† AND DOUGLAS A. FOUTCH†

3129e, 3129b Newmark Civil Engineering Laboratory, MC-250, 205 North Mathews Avenue, Urbana, IL 61801-2397, U.S.A.

SUMMARY

The seismic design provisions of most building codes in the United States specify ground motion parameters for various regions of the country and provide simple formulae to determine a distribution of lateral forces for which the structure should be designed. Although the code provisions are very simple to use, they oversimplify a complex problem and are based on many implicit assumptions which many designers may not appreciate. Furthermore, the reliability of the final design is not easily determined. This paper describes a reliability-based seismic design procedure for building structures. It is a performance-based design procedure which requires the designer to verify that a particular structural design satisfies displacement-based performance criteria. An equivalent system methodology and uniform hazard spectra are used to evaluate structural performance. The performance criteria are expressed in probabilistic terms, and deterministic design-checking equations are derived from these criteria. The design-checking equations incorporate design factors (analogous to load and resistance factors) which account for the uncertainty in the seismic hazard, the uncertainty in predicting site soil effects, and the approximate nature of the simplified models of the structure. The alternative procedure should enable designers to achieve code-specified target performance objectives for moderate and severe levels of earthquake excitation.

KEY WORDS: performance-based design; reliability-based design; multi-level seismic design; codes; probability

INTRODUCTION

The seismic design provisions of most building codes in the United States (U.S.) define a single 'design earthquake' as an earthquake which has a 10 percent probability of exceedance in 50 yr, and the codes provide the corresponding estimates of peak (or effective) ground acceleration or other related ground motion parameters for the various regions of the country. These ground motion parameters are then used in conjunction with simple formulae to determine a distribution of static lateral forces for which the structure should be designed. The resulting forces are '*equivalent* to the dynamic forces of an earthquake only in the sense that a structure designed to resist the code forces without overstress ought to be able — if the design is carefully executed to account for stress reversals, provide adequate member ductility, and provide connections of sufficient strength and resilience — to resist minor earthquakes without damage, resist moderate earthquakes without extensive structural damage, and resist major earthquakes without collapse'.[1] The various formulae used to determine the design lateral forces typically involve the use of one or more 'factors' or 'coefficients' to account for inelastic behaviour, relative importance of the structure, site soil effects, etc. The overall procedure is easy to apply, is based on years of experience and history, and is very familiar to designers.[2]

*Assistant Professor, Department of Civil & Environmental Engineering, University of Michigan, U.S.A.

†Professor in the Department of Civil Engineering, University of Illinois at Urbana-Champaign, Urbana, IL 61801, U.S.A.

CCC 0098–8847/96/121433–35

Received 27 June 1995
Revised 24 July 1996

Despite their simplicity and ease of use, the current seismic design provisions oversimplify a complex problem.[2] There are many inherent assumptions built into the approach which often are not well-understood or appreciated by designers. Furthermore, it is difficult to quantify the reliability of the final design. Although the design earthquake is selected based on probability, the various terms and 'factors' in the equations used to determine the design lateral forces are based on a significant amount of judgement and thus may contain much uncertainty.[3] Even if the factors were well-known and well-defined, the return period of the design earthquake provides little risk information on the performance of a structure designed for that earthquake.[4]

Recently, many studies have been carried out to investigate possible improvements to future seismic design provisions in the U.S. Suggested modifications include considering two or more levels of earthquake excitation,[5-7] incorporating structural reliability concepts,[2] using non-linear static push-over analyses,[2,7] and improving the techniques used to account for site soil effects on free-field ground motion.[8,9] This paper describes the key features of a proposed reliability-based seismic design procedure which attempts to address some of the shortcomings of current procedures and incorporates some of the modifications listed above. The proposed procedure uses uniform hazard spectra to define the seismic hazard at a site and an equivalent system methodology to evaluate the performance of the structure. The parameters of the equivalent system are calibrated using the results obtained from linear and non-linear static push-over analyses of the structure. Site soil effects are handled through the use of a recently proposed methodology that uses information on the mean shear wave velocity of site soils. Structural performance is quantified in terms of the probability of exceeding displacement-based performance criteria. Deterministic design equations are developed based on the probabilistic performance criteria; these equations include 'design factors' to account for the uncertainty in seismic hazard at the site, the uncertainty in predicting site soil effects, and the approximate nature of the equivalent system analysis methodology.

In the first few sections of the paper, some background information on uniform hazard spectra, the equivalent system methodology, the site soil factor methodology, and performance criteria for design is reviewed. Then, deterministic design-checking equations corresponding to some proposed performance criteria are presented. Finally, the proposed reliability-based design procedure is outlined in detail, and some example applications of the procedure are discussed.

UNIFORM HAZARD SPECTRA

Overview

Uniform hazard spectra present probabilistic information on the response of single-degree-of-freedom (SDOF) oscillators. Each ordinate of a particular uniform hazard spectrum curve has the same probability of exceedance associated with it.

The general concept of a uniform hazard spectrum is not new. For example, McGuire[10] describes a methodology for generating uniform hazard spectra for oscillators with linear elastic restoring forces, and Sewell and Cornell[11] extend the methodology to calculate the ordinates of uniform hazard spectra for oscillators with non-linear restoring forces. Both approaches use attenuation equations which describe the variation in oscillator response with parameters such as magnitude and source-to-site distance, and these equations are combined with the probability density functions for magnitude and distance to determine the SDOF response level corresponding to a target probability of exceedance. In the approach discussed by Sewell and Cornell, the ordinates of the hazard spectra for non-linear response are obtained using a procedure which scales the elastic response ordinates by reduction factors which are functions of the level of inelastic deformation, the frequency of the system, and other parameters.

In the present study, simulation is used to generate uniform hazard spectra. A specific site is selected, and artificial earthquake accelerograms are generated based on the seismicity of the surrounding region. Then, response spectra are calculated for each simulated record, and the statistics of the calculated responses are used to determine the probabilities of exceedance. This approach is more computationally intensive, but it eliminates the need for empirical relations describing the variation of spectral response (and/or spectral reduction factors) with magnitude, distance, etc.

The paragraphs below briefly summarize the important features and assumptions used in the simulation procedure and present examples of the uniform hazard spectra obtained in the study. Additional details can be found in Collins[12] and Collins *et al.*[13]

Simulation of earthquake ground motion records

The site selected for this study was near Los Angeles, California (U.S.A.). The geographical location of the site was 118° west longitude, 34° north latitude. The seismic hazard at the site was assumed to be dominated by the seismicity in the region within a 150 km radius of the site. The surrounding region was subdivided into 'seismic zones' as shown in Figure 1; within each zone, it was assumed that earthquakes were equally likely to occur anywhere. The seismic zones were based on the zones used by the U.S. Geological Survey[14–17] in its seismic hazard studies of the region. The soil conditions at the site were assumed to be consistent with the S_2 soil class defined in the NEHRP Recommended Provisions.[18]

Earthquakes were assumed to be exponentially distributed with respect to magnitude and interoccurrence time. These assumptions are consistent with the assumptions used by Algermissen *et al.*[14–17] The assumption of an exponential distribution of interoccurrence time implies that the number of earthquakes which occur within a given time span follows a Poisson distribution. Although the assumption of a Poisson distribution can be very restrictive and inappropriate,[19,20] the Poisson model is a 'sufficiently good' stochastic model for engineering applications for the Los Angeles metropolitan area.[21]

Within each zone, earthquakes were assumed to occur at discrete points; fault rupture lengths and fault orientations were not considered. Epicentral distance was the only source-to-station distance modelled in the simulation. The peak ground acceleration for each simulated record was determined using the regression equation proposed by Boore *et al.*[22,23] and this equation uses a more sophisticated measure of source-to-station distance defined as 'the closest horizontal distance from the station to the point on the earth's surface that lies directly above the rupture'. As an approximation, the epicentral distance was used instead of the 'closest horizontal distance'. Bender and Perkins[24] have observed that the seismic hazard at a site may be underestimated when this type of assumption is used.

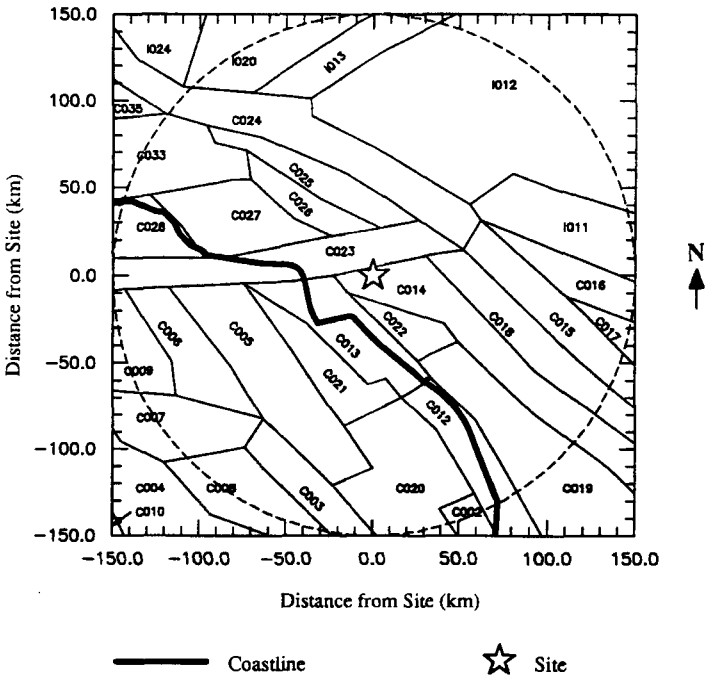

Figure 1. Seismic zones contributing to the seismic hazard at the site

The effects of directivity were not explicitly considered in the simulation procedure. As noted by Somerville *et al.*[25] and others, for sites near active faults, directivity effects can be significant. Somerville *et al.*[25] have recently proposed regression formulas for the ratio of fault-normal and fault-parallel ground motion and the ratio of fault-normal to average horizontal ground motion. Such formulae may be useful in future simulation studies where fault orientations and rupture lengths are considered.

The procedure used to generate each simulated record included provisions for modelling non-stationarity in both amplitude and frequency content. The non-stationary amplitude was modelled using the amplitude modulation function suggested by Clough and Penzien.[26] The frequency content of each simulated record was modelled using the regression equation for Fourier amplitude spectrum proposed by Trifunac.[27] This equation describes the variation of frequency content with magnitude, distance, and soil conditions. A very crude model for frequency modulation was used to approximate non-stationary frequency content. The frequency modulation model emphasized higher frequencies at the beginning of the record and lower frequencies at the end of the record. Such non-stationarity in frequency content is often observed in ground motion records.[28] However, it is recognized that this type of frequency modulation function cannot adequately simulate long-duration acceleration pulses such as those observed during recent earthquakes such as the 1994 Northridge Earthquake in southern California.

Uniform hazard spectra for linear elastic response

A total of 800 ten-year time periods were simulated, and 1292 artificial earthquake records were generated using the simulation procedure described above. Each simulated record was used to calculate the displacement response of a SDOF oscillator with a linear elastic restoring force. The governing equation of motion is

$$\ddot{d} + 2\zeta\omega\dot{d} + (\omega^2)d = -\ddot{x}_g \tag{1}$$

where d is the relative displacement of the mass of the oscillator with respect to the ground, x_g is the ground displacement, ω is the natural frequency of the oscillator, and ζ is the damping ratio. Dots indicate time derivatives. Responses were calculated at each of seven periods (0·1, 0·3, 0·5, 0·7, 1·0, 2·0 and 3·0 s) for a damping ratio of five percent ($\zeta = 0{\cdot}05$). The statistics of the responses were used to determine exceedance probabilities for various response levels, and this probabilistic information was used to calculate the ordinates of uniform hazard curves at each period for various target probabilities.

Figure 2(a) presents uniform hazard curves for four different target exceedance probabilities. The quantity shown on the y-axis is the elastic force coefficient, C_e, which is defined as the maximum spring force normalized by the weight of the oscillator. The probability associated with each curve is the probability of exceeding the indicated value of C_e. Figure 2(b) shows the same information as Figure 2(a) except that the y-axis now represents the maximum relative displacement, S_d, corresponding to the elastic force coefficient. The two quantities are related by

$$C_e = (\omega)^2 \frac{S_d}{g} = \left(\frac{2\pi}{T}\right)^2 \frac{S_d}{g} \tag{2}$$

where g is the acceleration due to gravity expressed in appropriate units and T is the natural period of the SDOF oscillator. Observe that C_e is equal to the spectral acceleration (pseudo-acceleration) normalized by gravity.

In general, uniform hazard spectra for linear elastic response do not have the same shape for all regions of the country.[29] Algermissen and Leyendecker[17] have proposed that an approximate uniform hazard curve can be constructed based on the knowledge of the ordinates at two periods: 0·3 and 1·0 s. This idea has been incorporated into the Appendix to Chapter 1 of the NEHRP Recommended Provisions[18] for constructing design spectra. Contour maps of the ordinates at 0·3 and 1·0 s are provided in the NEHRP Recommended Provisions for exceedance probabilities of 10 per cent in 50 yr and 10 per cent in 250 yr. Algermissen and

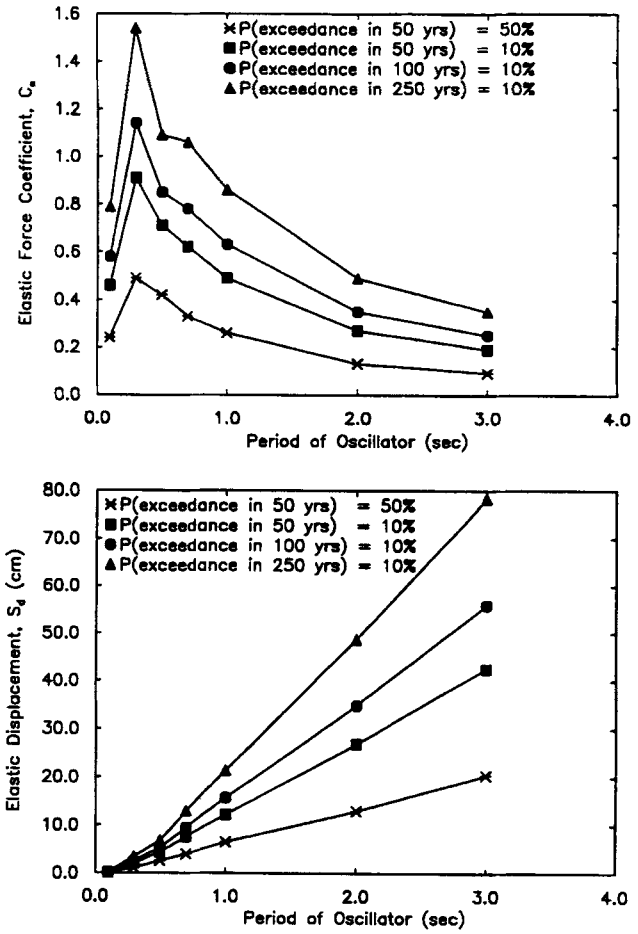

Figure 2. Uniform hazard spectra for elastic response. Both plots present the same probability information in two different ways. (a) Variation of elastic force coefficient with period at various probabilities of exceedance. (b) Variation of maximum relative displacement with period at various probabilities of exceedance

Leyendecker suggest that an approximate uniform hazard curve for linear elastic response can be constructed using

$$C_e^p(T) = \text{minimum}\left[C_e^p(T = 0{\cdot}3), \frac{C_e^p(T = 1{\cdot}0)}{T^n}\right] \tag{3}$$

where p is the exceedance probability, n is an exponent equal to 0·924 for California,[17] and $C_e^p(T)$ is the elastic force coefficient (or spectral acceleration) for the period T and exceedance probability p.

Figure 3 compares the approximate uniform hazard curves obtained using equation (3) with the curves obtained using the simulation procedure described earlier for two exceedance probabilities. The results compare favourably at an exceedance probability of 10 per cent in 50 yr, but the simulation results appear to give a lower estimate of hazard for periods below about 1 s for a probability level of 10 per cent in 250 yr. There are at least three possible reasons for the lower hazard estimates from the simulation results:

(1) The U.S. Geological Survey considered fault rupture lengths in their studies to determine values of $C_e(0{\cdot}3)$ and $C_e(1{\cdot}0)$, whereas the simulation procedure considered only point sources. As discussed earlier, neglecting fault rupture lengths and orientations can lead to lower hazard estimates at a site.

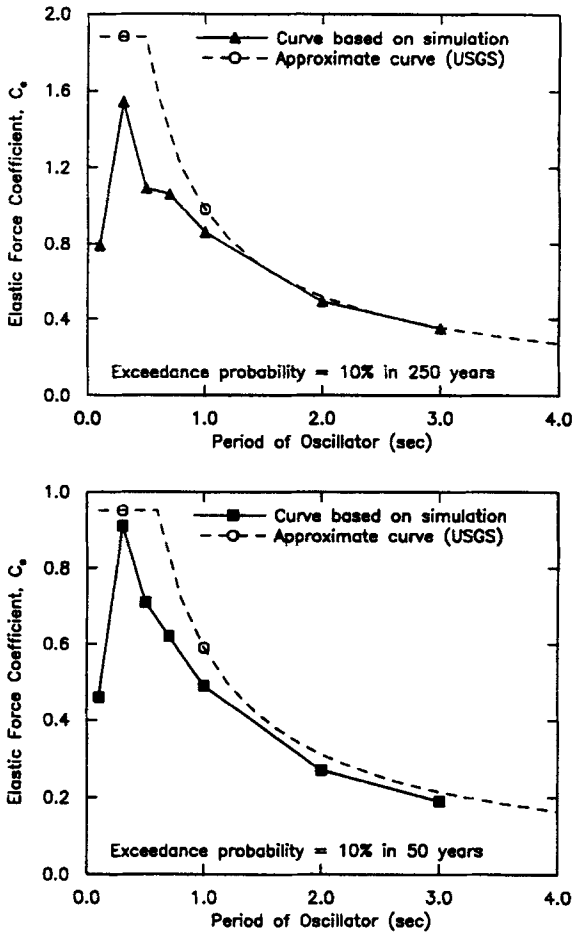

Figure 3. Comparison of the uniform hazard curves for linear elastic response obtained from the simulation study with approixmate uniform hazard curves constructed using the methodology proposed by Algermissen and Leyendecker. (a) Exceedance probability = 10 per cent in 250 yrs. (b) Exceedance probability = 10 per cent in 50 yrs

(2) Due to the limited number of simulations used (800 ten-year time periods), there is a large coefficient of variation (54 per cent) corresponding to the small exceedance probability of 10 per cent in 250 yr. The coefficient of variation describes the variability in estimating the probability of exceeding spectral response quantities. For a fixed number of simulations, the coefficient of variation increases as the exceedance probability decreases. The estimates of the hazard curve ordinates are only as good as the estimates of exceedance probability associated with the curve.
(3) The U.S. Geological Survey used a minimum magnitude of 4·6, whereas the simulation procedure was based on a minimum magnitude of 5·0. A higher minimum magnitude can result in lower predicted exceedance rates (probabilities).[24]

It should be noted that both the approximate curve and the curve based on simulation should be interpreted with caution. Many of the parameters and attenuation equations used in generating the curves are based on judgement and the limited amount of data in the historical catalog. As a result, the confidence in the hazard estimates decreases as the target exceedance probability decreases (i.e. as the exposure time increases).

Uniform hazard spectra for non-linear inelastic response

For each of the simulated accelerograms, the inelastic response of a SDOF oscillator was calculated. The oscillator was assumed to have a non-linear inelastic restoring force represented by the smooth hysteresis model discussed by Yeh and Wen.[30] The equation of motion for the oscillator is of the form

$$\ddot{d} + 2\zeta\omega\dot{d} + (\omega^2)f(\alpha, d, z) = -\ddot{x}_g \tag{4a}$$

$$f(\alpha, d, z) = \alpha d + (1 - \alpha)z \tag{4b}$$

where α is the post-to-preyield stiffness ratio (i.e. the strain-hardening ratio), d is the relative displacement of the mass with respect to the ground, x_g is the ground displacement, ω is the initial (linear elastic) natural frequency of the system, ζ is the damping ratio, z is the state variable describing the hysteretic behaviour of the restoring force, and dots denote time derivatives. A damping ratio of 0·05 and a post-to-preyield ratio of 0·05 were used in all analyses. The state variable z satisfies a differential equation of the form

$$\dot{z} = \frac{1}{\eta}\{A\dot{d} - \nu\beta|\dot{d}||z|^{n-1}z - \nu\gamma\dot{d}|z|^n\} \tag{5}$$

in which A, β, γ, ν, η and n are parameters which control the shape of the hysteresis loop. For this study, the parameters were chosen to simulate a bilinear hysteresis model; the values of the parameters were chosen to be as follows:

$$A = \eta = \nu = 1 \tag{6a}$$

$$n = 5 \tag{6b}$$

$$\beta = \gamma = \frac{1}{2d_y^n} \tag{6c}$$

The quantity d_y represents the yield displacement.

Analogous to the elastic force coefficient defined earlier, a non-dimensional yield force coefficient, C_y, can be defined as follows:

$$C_y = (\omega)^2\frac{d_y}{g} = \left(\frac{2\pi}{T}\right)^2\frac{d_y}{g} \tag{7}$$

At each period, the equation of motion for the non-linear SDOF oscillator was solved for discrete values of C_y for each simulated earthquake, and the statistics of the responses at each period and each value of C_y were used to estimate the probability of exceeding various values of displacement ductility. (Displacement ductility is defined as the maximum relative displacement divided by the yield displacement.)

There are two different ways to present uniform hazard information for non-linear inelastic response as shown in Figures 4 and 5. Each figure contains three plots. In Figure 4, each plot corresponds to a fixed value of ductility, and the variation in the required value of C_y with period is presented for various exceedance probabilities. The probability refers to the probability of exceeding the target ductility at the indicated value of C_y. In Figure 5, each plot corresponds to a fixed exceedance probability, and the variation in the required force coefficient (C_e or C_y) with period is presented. The significant trends shown in these figures are as follows:

(a) For a fixed target ductility and period, the probability of exceeding the target ductility decreases as the yield force increases (see Figure 4).
(b) For a fixed exceedance probability and period, the required yield force coefficient is a decreasing function of target ductility (see Figure 5).
(c) The curves in each plot in Figure 5 exhibit some of the same types of behaviour as constant-ductility non-linear response spectra calculated for individual earthquake records. As the period approaches zero, the curves for C_e and C_y appear to be converging for all target ductility values. In other words, the

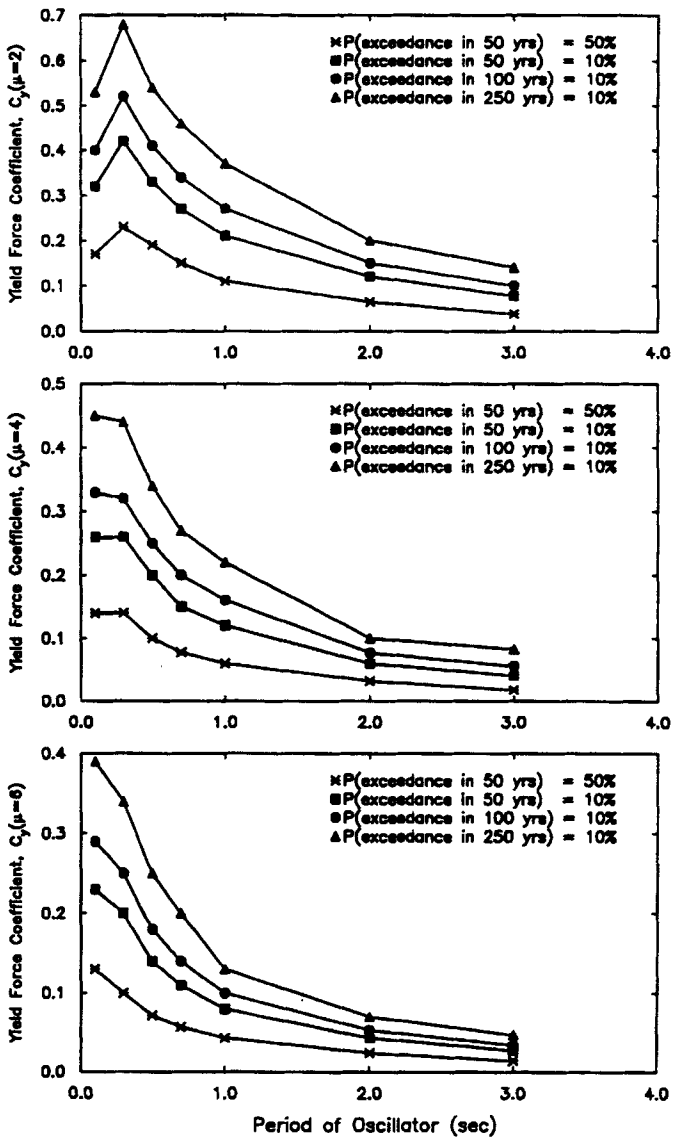

Figure 4. Uniform hazard spectra for non-linear response. Each plot presents the variation in the yield force coefficient with period for a fixed target ductility. (a) Target ductility = 2. (b) Target ductility = 4. (c) Target ductility = 6

ratio of C_e to C_y is approaching 1. As the period approaches infinity, the value of C_e/C_y appears to be approaching the target ductility ratio. For example, for an exceedance probability of 10 per cent in 50 yr and a period of 3·0 s, the ratios of C_e to C_y are about 2·4, 4·6, and 7 for ductilities of 2, 4, and 6, respectively.

(d) For a fixed value of yield force coefficient and period, the probability of exceedance decreases as the target ductility increases. This trend is not easily seen in Figures 4 and 5, but the simulation data do show this trend.

Implementation in design

For design purposes, it is impractical for seismic design codes to provide plots of uniform hazard spectra (for both linear and non-linear response) for a large number of sites in the U.S. and for various parameter

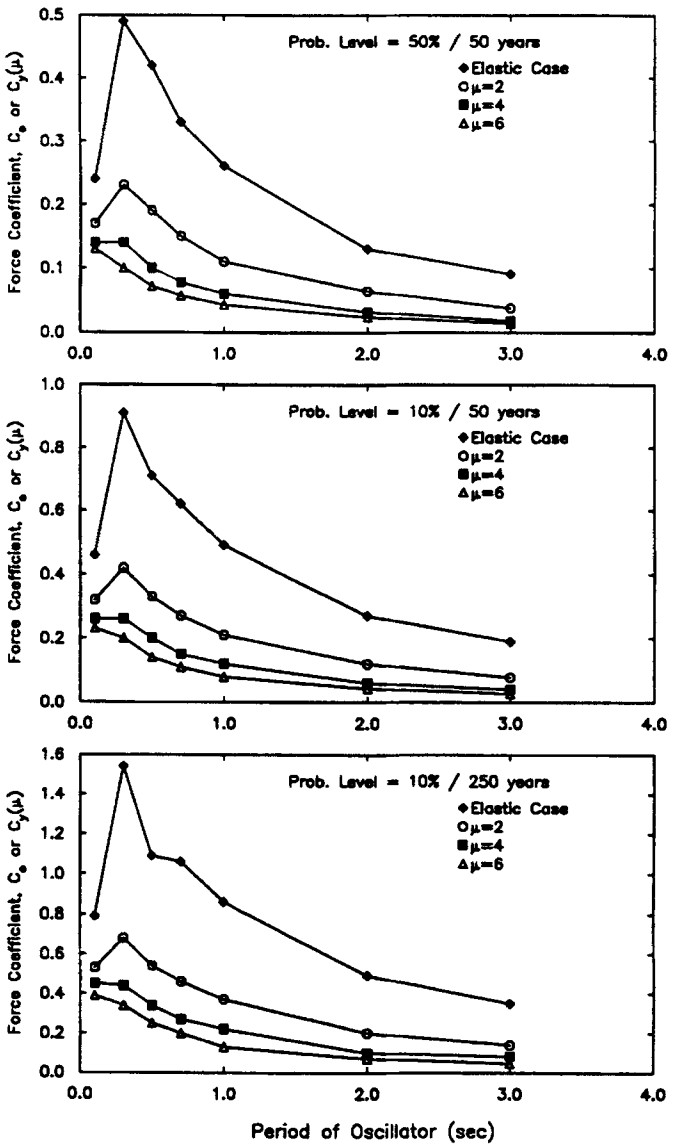

Figure 5. Uniform hazard spectra for non-linear response. Each plot presents the variation in the required force coefficient with period for a fixed exceedance probability. (a) Exceedance probability = 50 per cent in 50 yr. (b) Exceedance probability = 10 per cent in 50 yr. (c) Exceedance probability = 10 per cent in 250 yr

values (e.g. damping ratio, strain-hardening ratio). One alternative[31] might be to present uniform hazard data for elastic response (e.g. as proposed by Algermissen and Leyendecker[17]) and to prescribe formulas for spectral reduction factors to be used to determine the ordinates of uniform hazard curves for nonlinear response. The spectral reduction factor, as used herein, is defined as the ratio of C_e to C_y at period T for a target probability p, target ductility ratio μ, and strain-hardening ratio α, i.e.

$$R(p, T, \mu, \alpha) \equiv \frac{C_e^p(T)}{C_y^p(T, \mu, \alpha)} \tag{8}$$

This definition is analogous to the reduction factor often used in connection with response spectra for individual records.[32,33] In general, the value of R may also depend on the damping of the system and soil

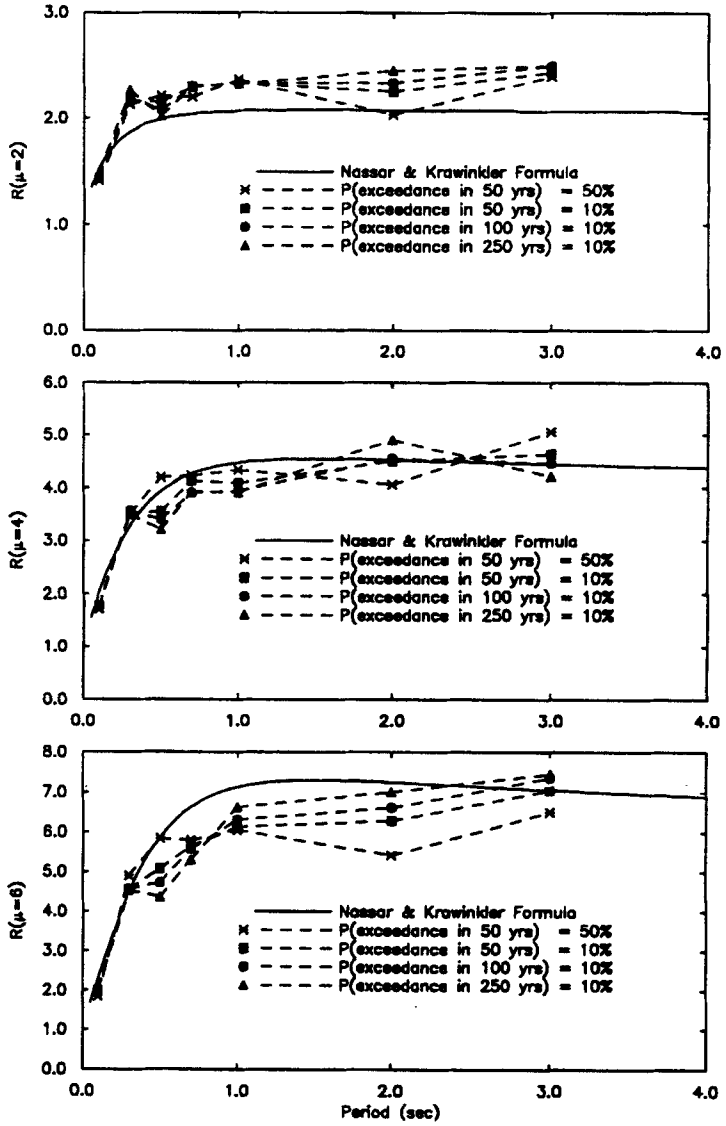

Figure 6. Comparison of spectral reduction factors for uniform hazard curves with reduction factors calculated using formula proposed by Nassar and Krawinkler. (a) Reduction factors for $\mu = 2$. (b) Reduction factors for $\mu = 4$. (c) Reduction factors for $\mu = 6$

conditions.[32] Figure 6 compares the values of R calculated from the simulation results using equation (8) with the values predicted by the formula proposed by Nassar and Krawinkler[33]

$$R(T, \mu, \alpha) \equiv (c(\mu - 1) + 1)^{1/c} \tag{9a}$$

$$c = c(T, \alpha) = \frac{T^a}{T^a + 1} + \frac{b}{T} \tag{9b}$$

where a and b are parameters which depend on the strain-hardening ratio α. Interpolating between the data provided by Nassar and Krawinkler for $\alpha = 2$ per cent and $\alpha = 10$ per cent, the values of a and b for $\alpha = 5$ per cent are 0·93 and 0·34, respectively; these values were used to construct the curves shown in Figure 6. As shown in Figure 6, for a fixed value of ductility, the value of R relating uniform hazard curves is not a strong

function of probability. Furthermore, the variation of R with T and μ for the uniform hazard results is somewhat different than the behaviour predicted by the formula proposed by Nassar and Krawinkler. Such differences are to be expected since the R factor proposed by Nassar and Krawinkler is based on an analysis of individual ground motion records without any explicit consideration of the probability of occurrence of the records. Additional research is needed to determine if the R factor relating uniform hazard results is dependent on the probability level and the characteristics of the seismic environment at a particular site.

Summary

The uniform hazard curves discussed herein provide examples of how probabilistic response information can be presented in a useful form for design purposes. The probability associated with a uniform hazard spectrum curve reflects the likelihood of earthquake occurrences as well as the severity of the earthquake ground motion when an earthquake occurs. It is important to emphasize that the simulation procedure described above contains many simplifying assumptions, and many of these assumptions are subject to debate. The uniform hazard curves presented herein are intended only to indicate general shapes and trends. In the development of uniform hazard spectra for design, it may be necessary to use more sophisticated techniques to model the seismic hazard in a particular region (e.g. the techniques used by the Working Group on California Earthquake Probabilities[34]) and/or a more sophisticated ground motion simulation procedure (e.g. the procedure suggested by Yeh and Wen[30]).

In order to use this information in the design of building structures, some method is needed to relate the response of a SDOF oscillator to the response of a multi-degree-of-freedom (MDOF) structure. This is the topic of the next section.

EQUIVALENT SYSTEM METHODOLOGY

The goal of the equivalent system methodology is to develop a SDOF equation of motion which can be used to estimate the displacement response at some selected 'significant' point on the MDOF structure. Several methodologies for developing SDOF models of MDOF systems have been proposed in the literature.[35-42] The starting point is the equation of motion of a two-dimensional MDOF cantilever-type structure subjected to horizontal base motion which can be written as

$$[M]\{\ddot{u}\} + [C]\{\dot{u}\} + \{R\} = -[M]\{1\}\ddot{u}_g \tag{10}$$

where $[M]$ is the mass matrix (assumed to be diagonal), $\{u\} = \{u(t)\}$ is the vector of lateral displacements (relative to the ground) at each floor (one displacement per floor), $[C]$ is the damping matrix, $\{R\} = \{R(t)\}$ is the restoring force vector, $\{1\}$ is the vector with all components equal to unity, and $u_g = u_g(t)$ is the ground displacement. Dots denote time derivatives. Using information obtained from a static push-over analysis, the above equation is reduced to a single equation describing the displacement response of the roof, $D = D(t)$, relative to the base. The resulting equation is of the form

$$\ddot{D} + 2\zeta\omega^*\dot{D} + (\omega^*)^2 G(D) = -P^*\ddot{u}_g \tag{11}$$

where P^* is analogous to a participation factor, ω^* is the effective frequency of the 'equivalent' system, ζ is the equivalent damping ratio, and $G(D)$ is a function describing the relationship between base shear and roof displacement during the push-over analysis. Formulae for some important quantities associated with equation (11) are presented in Appendix I of this paper; a detailed derivation is provided in the report by Collins *et al.*[13]

As shown in Appendix I, there are two vectors $\{\Psi_1\}$ and $\{\Psi_2\}$ used in the transformation of equation (10) to equation (11). The vector $\{\Psi_1\}$ is a normalized displacement profile obtained from a static push-over analysis of the structure. The vector $\{\Psi_2\}$ is used to reduce the MDOF equations to a single scalar equation. There are at least two possible choices for $\{\Psi_2\}$ as discussed by Collins[12] and Collins *et al.*[13] If $\{\Psi_2\} = \{\Psi_1\}$ is chosen, then equation (11) represents the equivalent SDOF equation derived based on the principle of virtual work.[26,39] This choice for $\{\Psi_2\}$ is the one typically found in the literature. Another choice is

$\{\Psi_2\} = \{1\}$ (i.e. all elements of the vector are equal to 1) which preserves the value of base shear.[12,13,42] Both choices of $\{\Psi_2\}$ will be discussed in subsequent sections. The choice of $\{\Psi_2\} = \{\Psi_1\}$ will be referred to as the 'virtual work' formulation of the equivalent system model, and the choice of $\{\Psi_2\} = \{1\}$ will be referred to as the 'base shear' formulation.

The equivalent system model described by equation (11) provides information on the roof displacement response. However, for seismic design purposes, the response quantity of interest is typically the maximum interstorey drift ratio among all floors. As described by Collins[12] and Collins *et al.*,[13] a factor β_{LG} can be defined using information on the displacement profile $\{\Psi_1\}$ used to formulate the equivalent system model. This factor can be used in conjunction with the maximum roof displacement, D_{max}, obtained from equation (11) to estimate the maximum interstorey drift ratio in the actual structure as follows:

$$(\Delta_L)_{max} = \beta_{LG} \frac{D_{max}}{H} \tag{12a}$$

$$\beta_{LG} = H\left[\frac{\Psi_{1,i} - \Psi_{1,i-1}}{h_i}\right]_{max} \tag{12b}$$

In equations (12a) and (12b), $(\Delta_L)_{max}$ is the estimate of the maximum interstorey drift ratio among all floors in the MDOF structure, D_{max} is the maximum roof displacement predicted by equation (11), H is the total height of the structure, and h_i is the height of the ith storey.

To validate the accuracy of the equivalent system methodology, the maximum roof displacement and maximum interstorey drift ratio for six two-dimensional steel building frames were calculated for both real and simulated earthquake records, and the results were compared to the estimates obtained using the equivalent system methodology for the same records. The six building frames consisted of a two-storey moment-resisting frame (MRF), a nine-storey MRF, a 12-storey MRF, an eight-storey MRF with vertical irregularity in mass and stiffness, a five-storey concentrically braced frame (CBF), and a five-storey dual system consisting of a MRF and a CBF. Detailed descriptions of the analysis models and the analysis techniques are provided in Collins[12] and Collins *et al.*;[13] a summary of the key results is provided below.

For each frame, different equivalent system models were developed to predict linear elastic response and non-linear inelastic response. Also, equivalent system models were developed for both choices of the vector $\{\Psi_2\}$ discussed earlier. For each frame, static push-over analyses were performed to calibrate the equivalent system parameters. (The UBC[43] lateral force distribution was used in all push-over analyses.) Figure 7 shows a set of four scatter plots which compare the maximum roof displacement and maximum interstorey drift ratio predicted by the 'linear' equivalent system models and the MDOF model of the nine-storey MRF. Figure 8 shows the same type of information for the nine-storey MRF, but the results are for non-linear inelastic response of the MDOF model (i.e. inelastic deformation occurred at one or more locations in the MDOF model). In each figure, the two scatter plots on the left compare predictions of roof displacement, and the two plots on the right compare predictions of maximum interstorey drift ratio. The two plots at the top of each figure show results for the virtual work formulation of the equivalent system model, and the two plots at the bottom show results for the base shear formulation. In each plot, a dot represents a comparison of the calculated response quantity for a particular earthquake record. If the dot is above the diagonal line, then the response of the equivalent system model for that record is larger than the response obtained from the MDOF model; if the dot is below the diagonal line, then the equivalent system response is smaller than that of the MDOF model. Tables I–IV summarize the statistics of the 'bias factors' for roof displacement and interstorey drift ratio for the nine-storey MRF as well as the other five structures. The bias factor for a particular response quantity (displacement or drift ratio) is the ratio of the response calculated using the MDOF model to the response calculated using the equivalent system model. The overall trends and results of the comparisons can be summarized as follows:

Linear elastic response—virtual work formulation. The equivalent system model based on $\{\Psi_2\} = \{\Psi_1\}$ predicts maximum roof displacement very well. The mean values of the bias factor for roof displacement are

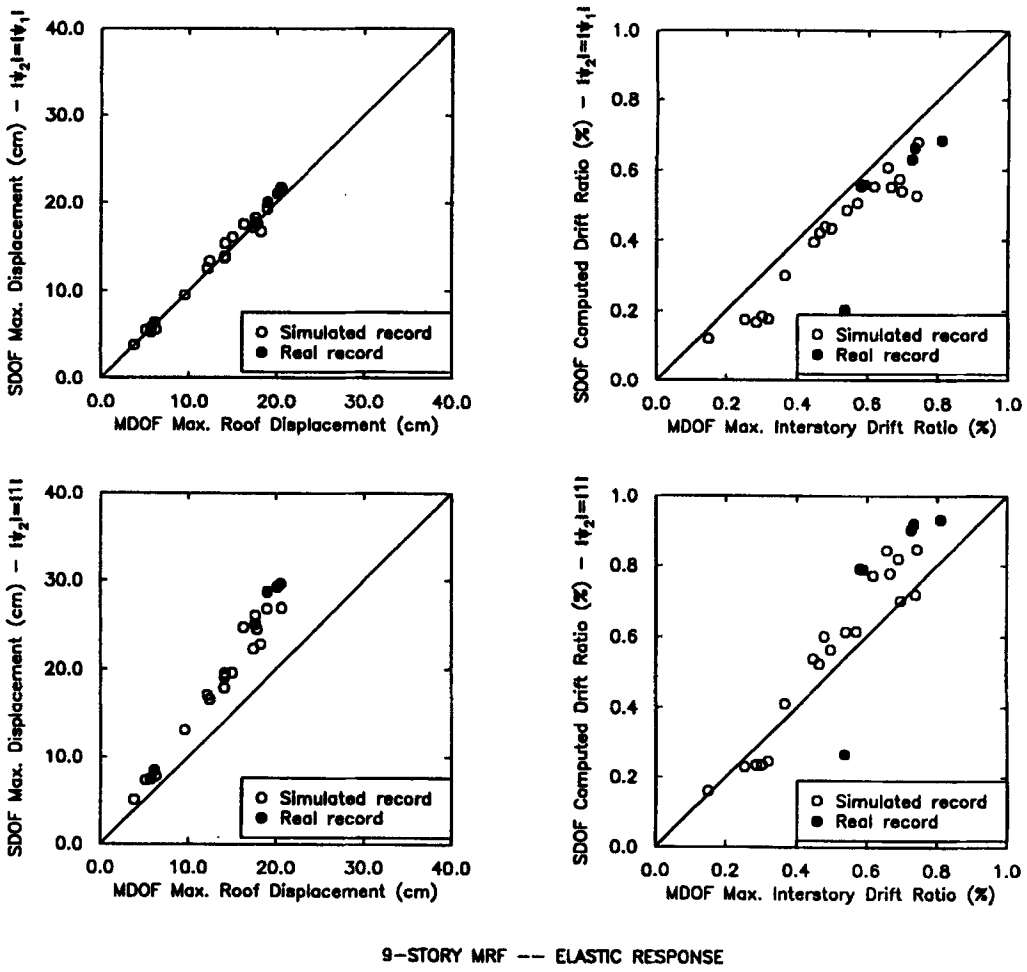

Figure 7. Scatterplot comparing maximum responses (roof displacement and interstorey drift ratio) predicted by equivalent SDOF models with responses obtained from an MDOF model of the nine-storey MRF. Response of MDOF model is linear elastic

all within the range 0·98–1·03. Furthermore, there is very little scatter in the data; the values of the standard deviation for the displacement bias factor are well below 0·1. The estimates of interstorey drift ratio using β_{LG} and the maximum roof displacement are too low. This implies β_{LG} is too small. The mean values of the bias factor for drift ratio range from 1·10 for the two-storey MRF to 1·44 for the 12-storey MRF. Also, there is more scatter in the data for drift. For example, for the nine-storey MRF, the standard deviation in the drift bias factor is 0·35 which is about 7 times higher than the standard deviation in the displacement bias factor (0·051). The higher scatter is to be expected since the basic equivalent system formulation is for roof displacement, and the conversion of roof displacement to maximum interstorey drift ratio is very approximate.

Linear elastic response—base shear formulation. The equivalent system model based on $\{\Psi_2\} = \{1\}$ overestimates roof displacement; this tends to compensate for the small value of β_{LG} and thus leads to better (slightly conservative) estimates of maximum interstorey drift ratio in most cases. For roof displacement, the mean values of the bias factor range from 0·73 to 0·79 for all structures except the two-storey MRF for which the mean bias factor is 0·91. The base shear formulation predicts larger roof displacements because the values of the ground motion scale factor P^* tend to be larger for the base shear formulation. For interstorey drift

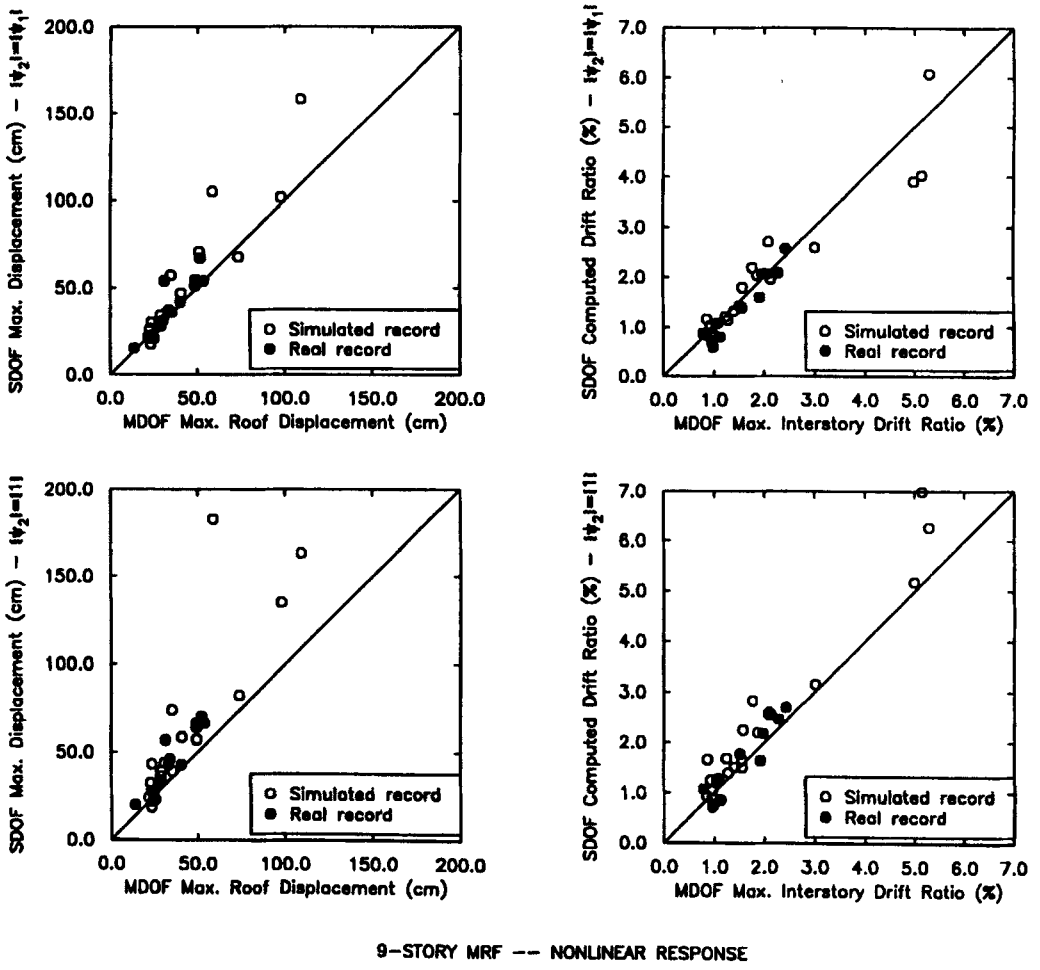

Figure 8. Scatterplot comparing maximum responses (roof displacement and interstorey drift ratio) predicted by equivalent SDOF models with responses obtained from a MDOF model of a nine-storey MRF. Response of MDOF model in non-linear

ratio, the mean values of the bias factor vary from 0·88 to 1·06. As observed for the virtual work formulation, there is more scatter in the drift bias factor than in the bias factor for roof displacement.

Nonlinear inelastic response—virtual work formulation. The equivalent system model based on $\{\Psi_2\} = \{\Psi_1\}$ provides reasonably good predictions of roof displacement. The mean bias factor for roof displacement ranges from 0·92 to 1·08, and the standard deviation in the bias factor ranges from 0·081 for the two-storey MRF to 0·19 for the five-storey CBF. For all but the eight-storey irregular MRF, the equivalent system underestimates the maximum interstorey drift ratio; the mean values of the bias factor range from 1·03 to 1·25. For the eight-storey MRF, the mean value of the drift bias factor is 0·91.

Nonlinear inelastic response—base shear formulation. As in the linear elastic case, the model based on using $\{\Psi_2\} = \{1\}$ tends to overpredict roof displacement; the mean bias factor ranges from 0·71 for the eight-storey MRF to 0·89 for the two-storey MRF and the five-storey CBF. For computing maximum interstorey drift ratio, the equivalent system model based on $\{\Psi_2\} = \{1\}$ provides better overall agreement with the MDOF results. Except for the eight-storey MRF, the mean bias factor for drift ratio ranges from 0·90 to 1·02. For the eight-storey irregular structure, the base shear formulation provides a very conservative estimate of the drift

Table I. Statistics for the bias factor, N_S^{DISP}, for estimates of maximum roof displacement for linear elastic response ($N_S^{DISP} = D_{MDOF}/D_{SDOF}$)

	$\{\Psi_2\} = \{1\}$ (Base shear)		$\{\Psi_2\} = \{\Psi_1\}$ (Virtual work)	
Structure	Mean	Std. dev.	Mean	Std. dev.
Two-storey MRF	0·91	0·018	1·01	0·025
Five-storey CBF	0·77	0·039	1·02	0·054
Five-storey dual system	0·79	0·039	1·03	0·053
Nine-storey MRF	0·73	0·041	0·98	0·051
Twelve-storey MRF	0·74	0·058	1·01	0·065
Eight-storey irregular MRF	0·75	0·066	1·03	0·062
All data except irregular structure	0·78	0·069	1·01	0·054
All data	0·78	0·070	1·01	0·055

Table II. Statistics for the bias factor, N_S^{DRIFT}, for estimates of maximum interstorey drift ratio for linear elastic response ($N_S^{DRIFT} = \Delta_{MDOF}/\Delta_{SDOF}$)

	$\{\Psi_2\} = \{1\}$ (Base shear)		$\{\Psi_2\} = \{\Psi_1\}$ (Virtual work)	
Structure	Mean	Std. dev.	Mean	Std. dev.
Two-storey MRF	0·99	0·095	1·10	0·12
Five-storey CBF	0·90	0·16	1·19	0·23
Five-storey dual system	0·91	0·17	1·18	0·22
Nine-storey MRF	0·96	0·27	1·29	0·35
Twelve-storey MRF	1·06	0·29	1·44	0·37
Eight-storey irregular MRF	0·88	0·14	1·21	0·18
All data except irregular structure	0·96	0·21	1·24	0·29
All data	0·95	0·21	1·24	0·28

Table III. Statistics for the bias factor, N_U^{DISP}, for estimates of maximum roof displacement for non-linear inelastic response ($N_U^{DISP} = D_{MDOF}/D_{SDOF}$)

	$\{\Psi_2\} = \{1\}$ (Base shear)		$\{\Psi_2\} = \{\Psi_1\}$ (Virtual work)	
Structure	Mean	Std. dev.	Mean	Std. dev.
Two-storey MRF	0·89	0·10	0·95	0·081
Five-storey CBF	0·89	0·15	1·08	0·19
Five-storey dual system	0·86	0·12	1·04	0·14
Nine-storey MRF	0·79	0·18	0·92	0·17
Twelve-storey MRF	0·79	0·12	0·95	0·13
Eight-storey irregular MRF	0·71	0·12	0·96	0·15
All data except irregular structure	0·84	0·14	0·99	0·16
All data	0·82	0·15	0·98	0·16

ratio as reflected by the mean bias factor of 0·67. For design purposes, such conservatism may be appropriate to discourage designs with significant vertical irregularity.

Simplified analyses using equivalent system models of MDOF building frames should not be expected to provide accurate results under all conditions. However, such analyses can provide useful information for

Table IV. Statistics for the bias factor, N_U^{DRIFT}, for estimates of maximum interstorey drift ratio for non-linear inelastic response ($N_U^{DRIFT} = \Delta_{MDOF}/\Delta_{SDOF}$)

	$\{\Psi_2\} = \{1\}$ (Base shear)		$\{\Psi_2\} = \{\Psi_1\}$ (Virtual work)	
Structure	Mean	Std. dev.	Mean	Std. dev.
Two-storey MRF	0·96	0·14	1·03	0·13
Five-storey CBF	1·02	0·21	1·25	0·25
Five-storey dual system	0·95	0·15	1·15	0·18
Nine-storey MRF	0·90	0·19	1·06	0·20
Twelve-storey MRF	0·92	0·16	1·11	0·20
Eight-storey irregular MRF	0·67	0·13	0·91	0·17
All data except irregular structure	0·95	0·17	1·12	0·21
All data	0·90	0·20	1·08	0·22

structural design.[37] Of the two formulations presented herein, the base shear formulation (i.e. using $\{\Psi_2\} = \{1\}$) appears to give conservative estimates of the displacement response of the structure. However, as long as the relative conservatism (or lack of conservatism) is properly accounted for in design, either formulation can be used.

MODELLING SITE SOIL EFFECTS

Most seismic design provisions provide design values of ground motion parameters for a specified reference soil condition. These parameters are typically scaled by site coefficients (or site soil factors) to obtain estimates of the ground motion parameters appropriate for the local soil conditions where the structure is to be built. For example, the NEHRP Recommended Provisions[18] defines four soil classes (S_1, S_2, S_3, and S_4) and the corresponding values of site coefficients (1·0, 1·2, 1·5 and 2·0). Recently, a new methodology for estimating site soil factors has been proposed[8,9] which uses information on the severity of ground motion shaking and the shear wave velocity of near-surface soils. This methodology is briefly summarized below, and is incorporated into the proposed reliability-based design procedure discussed later in this paper.

In the proposed methodology,[8,9] different site classes are distinguished based on the mean shear wave velocity of the top 30 m of soil at the site, the physical properties of the soil materials, and the thickness of the various constituent components of the soil profile. These site classes are shown in Table V. For each of the site classes, there is a corresponding range of values of the mean shear wave velocity. These ranges are based on observed correlations between physical properties of the soil and shear wave velocity.

Given information on the mean shear wave velocity of the top 30 m of soil at the site, the site soil factor (scaling factor) can be calculated using[8,9]

$$F = \left(\frac{v_{ref}}{v_{site}}\right)^{m(A_a, T)} \tag{13}$$

where v_{ref} is the mean shear wave velocity for the reference soil conditions, v_{site} is the mean shear wave velocity for the soil profile at the site, and $m(A_a, T)$ is an exponent which is a function of the period T of the structure and the severity of the input ground motion described by the parameter A_a. (The parameter A_a is the effective peak ground acceleration as defined in the NEHRP Recommended Provisions.[18]) Two period ranges are defined: a short-period range (T between 0·1 s up to about 0·4 s) and a mid-period range (T between 0·4 and 2 s). Based on regression analyses of data obtained from the Loma Prieta Earthquake (for which the value of A_a is estimated to be about 0·1 g), the values of m for the short-period range and the mid-period range are 0·35 and 0·65, respectively.[8,9]

Table V. Site classification scheme proposed by Borcherdt

Site class	Description	Mean shear wave velocity to a depth of 30 m (m/s)		
		Minimum	Average	Maximum
SC-Ia	Hard rocks (examples: Metamorphic rocks with very widely spaced fractures)	1400	1620	—
SC-Ib	Firm to hard rocks (examples: granites, igneous rocks, conglomerates, sandstones shales with close to widely spaced fractures)	700	1050	1400
SC-II	Gravelly soils and soft to firm rocks (examples: soft igneous sedimentary rocks, sandstones, shales, gravels, and soils with more than 20% gravel; minimum thickness = 10 m)	375	540	700
SC-III	Stiff clays and sandy soils (examples: loose to very dense sands, silt loams and sandy clays, and medium stiff to hard clays and silty clays; minimum thickness = 5 m)	200	290	375
SC-IVa	Non-special study soils (examples: loose submerged fills and very soft to soft clays and silty clays less than 37 m thick; minimum thickness = 3 m)	100	150	200
SC-IVb	Special study soils (examples: liquefiable soils, quick and highly sensitive clays, peats, highly organic clays, very high plasticity clays and soft soils more than 37 m thick; minimum thickness = 3 m)	Site-specific geotechnical investigations recommended for this class		

Prior to the 1994 Northridge Earthquake near Los Angeles, California (U.S.A.), there was very little information available to determine the functional relationship between m and A_a for higher levels of input ground motion. Laboratory results and numerical models were used to extrapolate the amplification factors derived from the Loma Prieta Earthquake to higher input ground motion levels. (Values of the exponent for discrete values of A_a are provided in the papers by Borcherdt.[8,9]) However, the Northridge Earthquake provided *in-situ* measurements of the response of various soil profiles to higher input ground motion levels. Preliminary analyses of the data indicate that the soil factor may not be strongly dependent on input ground motion level. In other words, the exponent m may be roughly constant for a wide range of input ground motion levels. It has been suggested[9] that, until the analyses of the Northridge data are completed, the site soil factors for $A_a = 0{\cdot}1\ g$ can be used for higher input ground motion levels. The results presented in this paper are based on this suggestion.

The proposed methodology attempts to reduce the ambiguity in defining soil classes and provides a more rigorous basis for quantifying site soil effects. However, there is a significant amount of uncertainty associated with this or any other scaling technique used to represent site soil effects. Analyses[12,13] indicate that the standard error of estimate in $\log(F)$ is about 0·21 for the short-period range and 0·18 for the mid-period range; the corresponding values of the coefficient of variation for F are 51 and 43 per cent, respectively. Clearly, such large uncertainty must be accounted for if reliable structural designs are to be achieved. This uncertainty is considered in the seismic design procedure presented later in this paper.

DISPLACEMENT-BASED PERFORMANCE CRITERIA

To formulate a reliability-based procedure, it is necessary to define the measures of structural performance (i.e. structural response quantities) to be considered, specify threshold values of the response quantities for each level of the design process, and define performance criteria in probabilistic terms. These decisions must be made by the code-writing organizations based on available technical data, engineering experience and judgment, and 'societal expectations regarding acceptable risk'.[7]

Most seismic design codes use interstorey drift (or interstorey drift ratio) as one measure of structural performance. The proposed procedure described herein also uses interstorey drift ratio. (Interstorey drift ratio is defined as the relative lateral displacement between two adjacent floors divided by the story height.) The threshold values of the interstorey drift ratio will vary depending on the level of ground motion excitation considered, the intended use of the structure, and the properties and performance characteristics of non-structural elements such as exterior cladding. Based on their review of seismic codes worldwide, Bertero *et al.*[5] observed that the maximum permissible interstorey drift ratio specified by codes for small to moderate earthquakes varies from 0·06 up to 0·6 per cent. For larger earthquakes, typical values of the maximum permissible interstorey drift ratio vary from 1 to 3 per cent.

In addition to interstorey drift ratio, the proposed procedure uses maximum global ductility as a measure of structural performance for 'large' earthquakes. (Global ductility is defined as the maximum roof displacement of the structure divided by the global yield displacement of the structure. The global yield displacement is determined from a static non-linear push-over analysis of the structure.) Such 'global' measures of damage are approximate and imperfect, but they can be useful in design applications. In the proposed procedure, maximum global ductility is used instead of a force reduction factor to determine the required strength of the structure to limit inelastic deformation during large earthquakes. Like the force reduction factors, the maximum global ductility threshold values specified by the code will depend on the structural framing system of the structure. The selection of these threshold values for various framing systems will necessarily involve a significant amount of engineering judgement and experience.

Current seismic code provisions generally do not use probability to define performance goals.[44] Instead, probability is used to define the return period of the 'design earthquake.' For example, the NEHRP Recommended Provisions[18] are based on a design earthquake for which the probability of exceedance is 10 per cent in 50 yr; the corresponding return period is about 475 yr. However, the return period of the design earthquake provides little risk information on the performance of a structure designed for that earthquake.[4] Wen, *et al.*[44] point out that 'it is by no means easy to obtain a consensus on the target levels of reliability even for traditional civil engineering structures'. Ideally, the target reliability is intended to reflect a balance between the level of structural safety and cost.[3] The design guidelines used by the U.S. Department of Energy[45] specify both the earthquake hazard levels and the target structural performance criteria to be considered in the design of various types of buildings. The performance criteria are expressed in terms of the annual probability of exceeding some measure of damage, and the probability values range from 10^{-3} to 10^{-5}. The Applied Technology Council[2] has suggested that appropriate target reliability levels for a dual-level design procedure might be 50 per cent in 50 yr for serviceability-related performance goals and 90 per cent in 250 yr for collapse prevention. These reliability levels correspond to annual *exceedance* probabilities of $1{\cdot}38 \times 10^{-2}$ and $4{\cdot}21 \times 10^{-4}$, respectively.

The target reliability levels mentioned above are presented only to give an indication of the 'order of magnitude' of such targets. It is beyond the scope of this paper to recommend specific target reliability levels to be used in design. Instead, the emphasis of this paper is to introduce a design procedure that can be used by designers to achieve the target reliability levels established by code-writing organizations in the future.

ANALYSIS OF UNCERTAINTY

Overview

This section presents the probabilistic performance criteria upon which the proposed design procedure is based and the corresponding deterministic design-checking equations that can be used to verify that

a structural design satisfies the criteria. Structural reliability methods and general probability theory were used to develop the deterministic design-checking equations. The derivations of the equations are discussed in detail in Collins[12] and Collins *et al.*[13] The deterministic design equations incorporate design factors (analogous to load and resistance factors) which account for the uncertainty in seismic hazard as well as the uncertainty in predicting site soil effects and the approximate nature of the equivalent system methodology. Values of the design factors are presented for various hypothetical performance criteria.

Uncertainty in prediction of linear elastic response

For small-to-moderate earthquakes, it may be feasible to specify a performance criterion which limits the maximum interstorey drift ratio, and it may also be appropriate to require the structure to remain linear elastic. For the present analysis, it is assumed that the code specifies a maximum interstorey drift ratio, Δ^{S}_{CODE}, and a target probability of exceedance, p_t. The actual interstorey drift ratio of the structure is Δ. Then, the performance criterion for interstory drift ratio might be stated as

$$P(\Delta > \Delta^{S}_{CODE}) \leqslant p_t \tag{14}$$

In words, the performance criterion in equation (14) requires the probability of exceeding some drift threshold *over some time interval* (e.g. 50 yr) to be less than or equal to p_t. If this performance criterion is adopted, then a deterministic design-checking equation of the form[12,13]

$$S_d(T^*) \leqslant \frac{H\Delta^{S}_{CODE}}{n\Omega_t F P^* \beta_{LG}} \tag{15}$$

can be used to verify that a particular design satisfies equation (14). In the above equation, S_d is the elastic spectral displacement obtained from the uniform hazard curve corresponding to the target probability p_t, T^* is the period of the equivalent system model for linear elastic response, F is the site soil factor calculated using equation (13), n is the bias factor (i.e. the value of the bias factor N_S^{DRIFT} assumed for design purposes), H is the total structure height, β_{LG} and P^* are equivalent system parameters, and Ω_t is the design factor which accounts for the fact that the soil factor, the bias factor, and the elastic spectral displacement are all random variables.

The design factor Ω_t can be calibrated for a given target exceedance probability using information on the distributions of the three random variables. Table VI presents values of Ω_t for target exceedance probabilities of 50 per cent in 50 yr and 10 per cent in 50 yr. The values of Ω_t are based on the following assumptions regarding the values of n and F used in equation (15). The bias factor (n) is assumed to be 1·0, and the bias statistics for the equivalent system formulation using $\{\Psi_2\} = \{1\}$ are used. For demonstration purposes, the variability (i.e. coefficient of variation, COV) in the bias factor is chosen to be the *average* COV for all six structures discussed earlier. The value of F is the value calculated using equation (13) assuming $A_a = 0{\cdot}1$. (As noted earlier, the possible dependence of the soil factor on A_a is not considered herein.) The design value of the elastic force coefficient, C_e, (which is proportional to S_d) is the value which has a probability of exceedance equal to p_t. The results in Table VI can be summarized as follows:

(a) The value of the design factor at each period is independent of the site soil conditions. (It can be shown mathematically that this must be true.)
(b) The values of the design factor for an exceedance probability of 10 per cent in 50 yr are, in general, slightly larger (by less than 5 per cent) than the values for an exceedance probability of 50 per cent in 50 yr. The relatively small increase in the design factor is a consequence of the way in which the design factor is defined. The design value of C_e (or S_d) depends on the target probability of exceedance. Therefore, changes in the hazard level (i.e. changes in the value of p_t) are directly reflected in the value of C_e. The primary purpose of the design factor is to account for the variability in the bias factor and the soil factor which is relatively small compared to the variability in C_e (or S_d).
(c) The design factors vary with the period of the structure. This is a consequence of the relative dispersion of the hazard at each period and the differences in the soil factor uncertainty for different period ranges.

Table VI. Values of the design factor Ω_t used for predicting linear elastic response

			Design factor for various values of site shear wave velocity. v^* (m/s)							
					$v = v_{ref} = 540$					
Period (s)	$\sigma_{\log F}$	Design value of C_e	$v = 1620$	$v = 1050$	$(1{\cdot}0)\sigma_{\log F}$	$(0{\cdot}5)\sigma_{\log F}$	$(0{\cdot}01)\sigma_{\log F}$	$v = 450$	$v = 290$	$v = 150$
Target exceedance probability (p_t) = 50% *in* 50 yr										
0·1	0·21	0·24	1·25	1·25	1·25	1·02	0·95	1·25	1·25	1·25
0·3	0·21	0·49	1·28	1·28	1·28	1·02	0·95	1·28	1·28	1·28
0·5	0·18	0·42	1·24	1·24	1·24	1·02	0·96	1·24	1·24	1·24
0·7	0·18	0·33	1·19	1·19	1·19	1·01	0·96	1·19	1·19	1·19
1·0	0·18	0·26	1·14	1·14	1·14	0·98	0·93	1·14	1·14	1·14
2·0	0·18	0·13	1·15	1·15	1·15	1·00	0·95	1·15	1·15	1·15
3·0	0·18	0·091	1·13	1·13	1·13	0·99	0·94	1·13	1·13	1·13
Target exceedance probability (p_t) = 10% *in* 50 yr										
0·1	0·21	0·46	1·29	1·29	1·29	1·02	0·95	1·29	1·29	1·29
0·3	0·21	0·91	1·31	1·31	1·31	1·03	0·95	1·31	1·31	1·31
0·5	0·18	0·71	1·26	1·26	1·26	1·03	0·96	1·26	1·26	1·26
0·7	0·18	0·62	1·21	1·21	1·21	1·01	0·96	1·21	1·21	1·21
1·0	0·18	0·49	1·19	1·19	1·19	1·01	0·95	1·19	1·19	1·19
2·0	0·18	0·27	1·15	1·15	1·15	0·99	0·94	1·15	1·15	1·15
3·0	0·18	0·19	1·15	1·15	1·15	0·99	0·94	1·15	1·15	1·15

*The value of the soil factor is calculated for a *constant* value of A_a

(d) For the assumed *reference* soil conditions, some of the uncertainty in site soil effects is implicitly accounted for in the simulation procedure used to generate the uniform hazard spectra. Several of the regression equations used in the simulation procedure incorporate variables to account for site soil effects, although the values of the variables and the rationale behind them differ in each case. It is difficult to quantify by how much the uncertainty in the soil factor can be reduced for the reference soil conditions. In Table VI, two lower values of $\sigma_{\log F}$ are considered for reference soil conditions. As expected, reducing the uncertainty in the soil factor can significantly reduce the values of the design factors. For example, at a period of 0·3 s and $p_t = 50$ per cent in 50 yr, reducing $\sigma_{\log F}$ by 50 per cent reduces the design factor by about 20 per cent.

Uncertainty in prediction of nonlinear inelastic response

For large earthquakes, it may be impractical and uneconomical to design a building structure which will remain essentially elastic. Thus, some non-linear response behaviour may be considered acceptable. However, limits on the non-linear response behaviour are necessary to preserve structural integrity, reduce structural damage, and avoid the loss of life. In the subsequent sections, it is assumed that the seismic design code specifies both a maximum interstorey drift ratio (Δ^{U}_{CODE}) and a maximum global ductility ratio (μ_{CODE}). Also, it is assumed that there is a target probability of exceedance associated with both limits.

Global ductility, as used herein, is defined as

$$\mu_{MDOF} \equiv \frac{D_{max}}{D_y} \tag{16}$$

where D_{max} is the maximum lateral roof displacement of the MDOF structure and D_y is the global yield displacement of the structure obtained from a static push-over analysis of the structure. The performance criterion for global ductility is assumed to be

$$P(\mu_{MDOF}@D_y > \mu_{CODE}) \leqslant p_t \tag{17}$$

where the notation '@ D_y' emphasizes the dependence of the non-linear response on the global yield displacement. If a value D^t_y can be found such that the probability of exceeding μ_{CODE} is *equal* to p_t, then the structural design would satisfy the performance criterion for global ductility if $D_y \geqslant D^t_y$. The deterministic design equation corresponding to this requirement is[12,13]

$$D_y \geqslant \Omega^F_t P^* F g \left(\frac{T^*}{2\pi}\right)^2 C_y(\mu_t) \quad \text{where} \quad \mu_t = \frac{\mu_{CODE}}{\Omega^\mu_t n^{DISP}_U} \tag{18}$$

where Ω^F_t is the design factor accounting for the variability in the soil factor, Ω^μ_t is the design factor accounting for the random nature of the bias factor N^{DISP}_U, n^{DISP}_U is the mean bias factor, P^* is the ground motion scale factor for the equivalent system model, F is the soil factor calculated using equation (13), g is the acceleration due to gravity, T^* is the period of the equivalent system model for non-linear response, and $C_y(\mu_t)$ is the yield force coefficient at $T = T^*$ obtained from the uniform hazard spectrum curve for non-linear response corresponding to μ_t and p_t. Unlike equation (15) in which one design factor is used to cover the uncertainty in both the soil factor and the bias factor, equation (18) uses a distinct design factor for each of these sources of uncertainty. The derivation of equation (18) presented by Collins *et al.*[13] shows that the two sources of uncertainty must be treated separately for the non-linear case.

To control the maximum interstorey drift, the performance criterion can be stated as

$$P(\Delta@D_y > \Delta^U_{CODE}) \leqslant p_t \tag{19}$$

where Δ is the maximum interstorey drift ratio among all storeys in the actual structure and Δ^U_{CODE} is the target maximum interstorey drift ratio defined by the code for severe earthquake conditions. The deterministic design-checking equation corresponding to equation (19) is[12,13]

$$\Delta^U_{CODE} \geqslant \mu' \frac{\beta_{LG}}{H} \Omega^\Delta_t n^{DRIFT}_U D_y \tag{20}$$

Table VII. Values of the design factor Ω_t^F used for predicting non-linear inelastic response

		Target ductility = 2		Target ductility = 3		Target ductility = 4		Target ductility = 6	
Period (s)	$\sigma_{\log F}$	Value of $C_y(\mu = 2)$ from UHS	Ω_t^F	Value of $C_y(\mu = 3)$ from UHS	Ω_t^F	Value of $C_y(\mu = 4)$ from UHS	Ω_t^F	Vaue of $C_y(\mu = 6)$ from UHS	Ω_t^F
Target exceedance probability (p_t) = 10%/50 yr									
0·1	0·21	0·32	1·43	0·28	1·43	0·26	1·41	0·23	1·42
0·3	0·21	0·42	1·45	0·31	1·41	0·26	1·40	0·20	1·39
0·5	0·18	0·33	1·32	0·24	1·28	0·20	1·27	0·14	1·27
0·7	0·18	0·27	1·29	0·20	1·29	0·15	1·26	0·11	1·27
1·0	0·18	0·21	1·27	0·16	1·24	0·12	1·25	0·080	1·29
2·0	0·18	0·12	1·30	0·076	1·27	0·060	1·28	0·043	1·32
3·0	0·18	0·078	1·25	0·053	1·24	0·041	1·22	0·027	1·27
Target exceedance probability (p_t) = 10%/100 yr									
0·1	0·21	0·40	1·43	0·35	1·43	0·33	1·42	0·29	1·43
0·3	0·21	0·52	1·46	0·39	1·42	0·32	1·40	0·25	1·40
0·5	0·18	0·41	1·32	0·31	1·28	0·25	1·27	0·18	1·27
0·7	0·18	0·34	1·29	0·25	1·29	0·20	1·26	0·14	1·27
1·0	0·18	0·27	1·27	0·20	1·24	0·16	1·25	0·10	1·30
2·0	0·18	0·15	1·30	0·097	1·27	0·077	1·28	0·053	1·31
3·0	0·18	0·10	1·25	0·069	1·24	0·056	1·21	0·034	1·28
Target exceedance probability (p_t) = 10%/250 yr									
0·1	0·21	0·53	1·43	0·47	1·43	0·45	1·42	0·39	1·43
0·3	0·21	0·68	1·46	0·53	1·42	0·44	1·40	0·34	1·40
0·5	0·18	0·54	1·32	0·42	1·28	0·34	1·27	0·25	1·27
0·7	0·18	0·46	1·29	0·33	1·30	0·27	1·27	0·20	1·27
1·0	0·18	0·37	1·27	0·29	1·24	0·22	1·25	0·13	1·30
2·0	0·18	0·20	1·30	0·13	1·27	0·10	1·28	0·070	1·31
3·0	0·18	0·14	1·25	0·10	1·24	0·083	1·21	0·047	1·27

where Ω_t^A is the design factor accounting for the random nature of the bias factor N_U^{DRIFT}, n_U^{DRIFT} is the mean bias factor, β_{LG} is the factor used to convert the global drift ratio to interstorey drift ratio in the equivalent system methodology, H is the total structure height, and μ' is a ductility corresponding to D_y. The ductility μ' is interpreted as follows: for the equivalent system model with a yield displacement $D_{y,ES}$ equal to D_y, the probability that the maximum ductility of the equivalent system model will exceed μ' is equal to p_t.

Table VII presents the values of the design factor Ω_t^F for three target probabilities of exceedance and four target ductilities. This factor is a multiplier which is used in conjunction with the design yield force coefficient, $C_y(\mu)$, and the design site soil factor as shown in equation (18). In this study, the design value of $C_y(\mu)$ is chosen to be the value for which the probability of exceeding μ is equal to the target probability p_t under consideration. The value of the site soil factor (F) is the value calculated using equation (13) assuming $A_a = 0{\cdot}1$. (The possible dependence of F on A_a is not considered.) The results shown in Table VII can be summarized as follows:

(a) The value of Ω_t^F is period dependent. The same type of period dependence was observed for the design factor discussed earlier in connection with linear elastic response. The values of Ω_t^F range from 1·21 at $T = 3{\cdot}0$ s to 1·46 at $T = 0{\cdot}3$ s.

(b) For the range of exceedance probabilities considered, the values of the design factor do not vary significantly with target exceedance probability at a fixed period. The variation is typically less than

1 per cent. This small variation is a result of the way in which the design factor is defined. In many applications (e.g. load and resistance factor design[46]), the design factor is applied to some nominal design value of the 'load' or 'load effect', and the same nominal value is used when calibrating the 'load factor' (design factor) at various exceedance probabilities. When this is done, the value of the design factor can change dramatically for different target probabilities of exceedance. In the present study, the design factor is applied to a design value of $C_y(\mu)$ which changes with the value of p_t under consideration. Thus, the design factor would be expected to exhibit smaller fluctuations as p_t is changed.

(c) For a fixed period, the design factor does not, in general, vary significantly with ductility for ductilities between 2 and 6. The maximum variation is about 6 per cent. This is significant for code implementation since it implies that a single value of the design factor can be specified at each period which is valid for a range of ductilities.

Table VIII shows the sensitivity of the design factor Ω_t^F to the level of uncertainty in the site soil factor. Three values of $\sigma_{\log F}$ are considered. Results are presented for two exceedance probabilities and a target ductility of 4. As expected, reducing the uncertainty in the site soil factor can result in a significant reduction in the value of the design factor. Reducing $\sigma_{\log F}$ by 50 per cent can reduce the value of Ω_t^F by as much as 23 per cent.

To calibrate values of Ω_t^μ and Ω_t^Δ for both N_U^{DISP} and N_U^{DRIFT}, respectively, information on the probability distribution functions for ductility at *fixed* values of yield displacement are required. (These functions are conditional probability functions which describe the uncertainty in ductility demand given a fixed value of yield displacement.) Due to a lack of adequate information on these distribution functions, values of Ω_t^μ and Ω_t^Δ were not calculated for various values of p_t at each period as was done for Ω_t^F. However, based on some *very approximate* calculations, it appears that, in general, the values of Ω_t^μ and Ω_t^Δ range from 1·1 to 1·4. The values of both of these design factors would be expected to be smaller than the values of Ω_t^F since the values of the coefficient of variation for the bias factors are on the order of 20 per cent and the coefficient of variation in the site soil factor is 40–50 per cent. The approximate calculations indicate that the choice of the equivalent

Table VIII. Variation in design factor Ω_t^F with level of uncertainty in the site soil factor

Period (s)	$\sigma_{\log F}$	Value of $C_y(\mu)$ from UHS	Design factors for *Reference* soil condition for different levels of uncertainty in soil factor (target ductility = 4)		
			$\sigma_{\log F}$	$(0{\cdot}5)\sigma_{\log F}$	$(0{\cdot}01)\sigma_{\log F}$
Target exceedance probability (p_t) = 10%/50 yr					
0·1	0·21	0·26	1·41	1·09	1·0
0·3	0·21	0·26	1·40	1·09	1·0
0·5	0·18	0·20	1·27	1·06	1·0
0·7	0·18	0·15	1·26	1·06	1·0
1·0	0·18	0·12	1·25	1·06	1·0
2·0	0·18	0·060	1·28	1·07	1·0
3·0	0·18	0·041	1·22	1·05	1·0
Target exeedance probability (p_t) = 10%/250 yr					
0·1	0·21	0·45	1·42	1·09	1·0
0·3	0·21	0·44	1·40	1·09	1·0
0·5	0·18	0·34	1·27	1·06	1·0
0·7	0·18	0·27	1·27	1·06	1·0
1·0	0·18	0·22	1·25	1·06	1·0
2·0	0·18	0·10	1·28	1·06	1·0
3·0	0·18	0·083	1·21	1·05	1·0

system formulation (i.e. virtual work or base shear) does not make a significant difference in the values of Ω_t^{μ} and Ω_t^{Δ}. This is an expected result based on the bias statistics discussed earlier; for each of the bias factors, the values of the coefficient of variation for both formulations are comparable.

OUTLINE OF DESIGN/ANALYSIS PROCEDURE

Overview

The intent of most seismic design provisions in the U.S. is to provide design and analysis procedures which, if used, should result in structural designs which will resist small earthquakes without damage, resist moderate earthquakes without major structural damage, and resist large earthquakes without collapse.[2] The current provisions attempt to achieve all three performance objectives by specifying only one design earthquake level. However, such a single-level design criterion cannot provide consistent damage control and protection from collapse. A dual-level design procedure which specifies two earthquake levels and two limit states would be an improvement.[5] (A limit state represents a state of undesirable structural behaviour[47] and may be based on functional requirements or collapse considerations.[46]) The proposed procedure is such a dual-level design procedure. The first level (stage) of design is associated with a *serviceability* limit state. The design and analysis procedures in this first stage attempt to ensure elastic (or nearly elastic) response of a structure during small-to-moderate earthquakes. The second stage of design is associated with an *ultimate* limit state. The second stage focuses on controlling the non-linear inelastic behaviour which is expected to occur during extreme (relatively rare) earthquake events. The proposed procedure incorporates some of the ideas for displacement-based seismic design suggested by R.D. Bertero and V.V. Bertero[6] and Qi and Moehle.[37] The basic steps in each stage of the dual-level procedure are summarized in the subsections below and in the flowcharts presented in Figures 9 and 10.

Design and analysis procedure for the serviceability limit state

The procedure for the serviceability limit state attempts to focus simultaneously on the relationship between stiffness and strength in satisfying the serviceability limit state criterion. The serviceability limit state focuses on ensuring elastic (or nearly elastic) behaviour of the structure while controlling interstorey drift. Given a threshold value of interstorey drift ratio for the serviceability limit state ($\Delta_{\text{CODE}}^{\text{S}}$) and a target exceedance probability (p_t), the performance criterion is as stated in equation (14). The steps for this level of design are outlined below. (Most of the calculations in Steps 1–10 are not needed if a preliminary structural design exists.)

1. Determine the general layout of the structure. Determine the number of storeys, the storey heights, the total height of the structure (H), and the estimated floor weights and loads to be considered in the seismic design of the structure.
2. Calculate the short-period and mid-period values of the site soil factor, F, using equation (13). (In this procedure, it is assumed that the exponent m is not a function of the level of input ground motion. The values of m for $A_a = 0{\cdot}1$ are to be used.)
3. Using the estimated floor weights, formulate the lumped mass matrix $[M]$ for the structure.
4. For the initial iteration of the design process to determine preliminary member sizes, assume a normalized displacement profile $\{\Psi_1\}$. If $\{\Psi_1\}$ is assumed to be linear, then the corresponding value of β_{LG} is 1. However, since β_{LG} is always larger than 1, a larger value of β_{LG} (for example, 1.2) can be assumed for the initial iteration. (An alternate choice of $\{\Psi_1\}$can be used if desired.)
5. Calculate L^*, M^*, P^*, and β_{LG} (if necessary) using the assumed shape vector $\{\Psi_1\}$ as follows:

$$M^* = \{\Psi_2\}^T[M]\{\Psi_1\} \tag{21}$$

$$L^* = \{\Psi_2\}^T[M]\{1\} \tag{22}$$

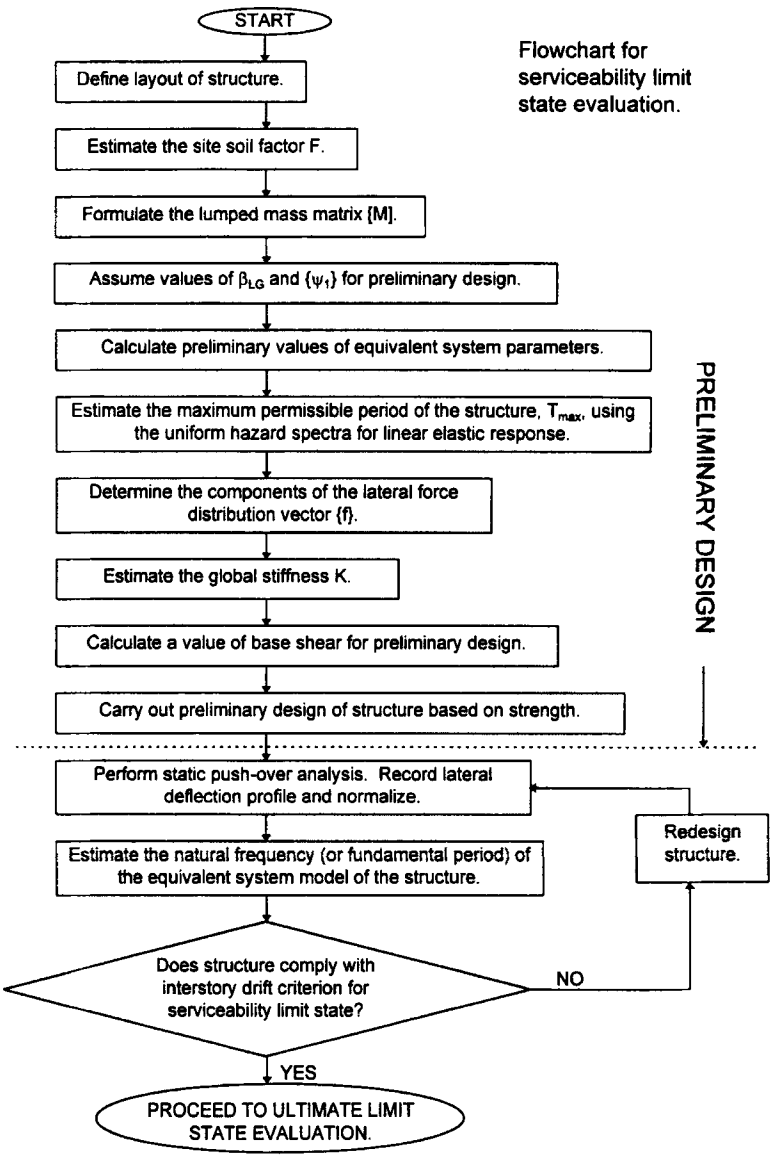

Figure 9. Flowchart summarizing the steps in the serviceability limit state evaluation

$$P^* = L^*/M^* \tag{23}$$

$$\beta_{LG} = H\left[\frac{\Psi_{1,i} - \Psi_{1,i-1}}{h_i}\right]_{max} \tag{24}$$

If the base shear formulation of the equivalent system model is used, then $\{\Psi_2\} = \{1\}$. If the virtual work formulation is used, then $\{\Psi_2\} = \{\Psi_1\}$.

6. Determine the maximum permissible fundamental period, T^*_{max}, based on the code-specified drift limit, Δ^S_{CODE}, as follows. Use the uniform hazard spectrum curve for spectral displacement (for a target exceedance probability p_t) to find the spectral displacement, S_d, such that

$$S_d(T^*_{max}) = \frac{H\Delta^S_{CODE}}{n\Omega_t F P^* \beta_{LG}} \tag{25}$$

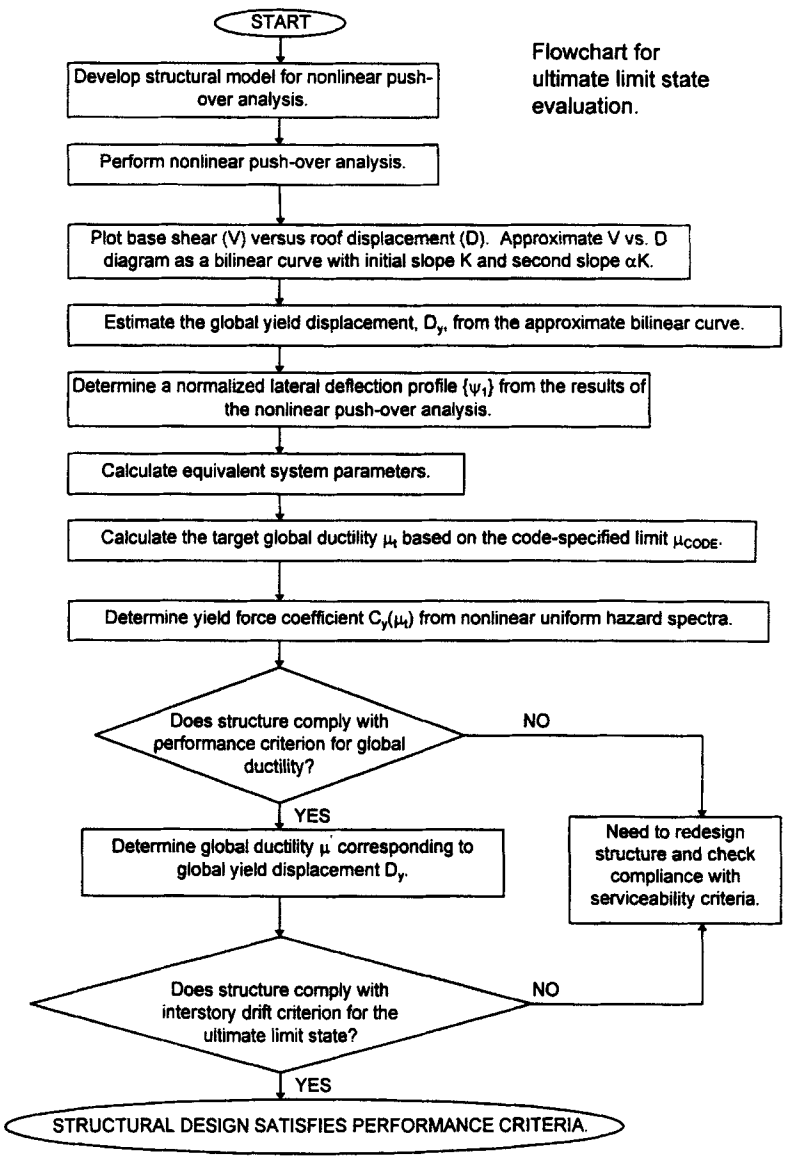

Figure 10. Flowchart summarizing the steps in the ultimate limit state evaluation

where Ω_t is the design factor corresponding to the target exceedance probability p_t for the serviceability limit state. Since F and Ω_t depend on period, equation (25) must be solved by trial and error. The spectral displacement generally increases with period; thus, the above condition imposes an upper limit on the period T^* of the equivalent system model and hence imposes an upper limit on the structure's fundamental period.

7. Determine the normalized lateral force distribution, $\{f\}$, to be used in design. If $\{f\}$ is a function of the structure's period (e.g. the UBC[43] force distribution), then $T^* = T^*_{max}$ can be used for the first iteration. Alternatively, period estimates from empirical formulae in the code can be used.
8. Determine a preliminary value of global stiffness, K, using

$$K = \frac{4\pi^2}{(T^*)^2} \frac{M^*}{\{\Psi_2\}^T\{f\}} \tag{26}$$

9. Determine a preliminary value of the design base shear using

$$V = KD^{\text{DRIFT}} = K[n\Omega_t FP^* S_d] \tag{27}$$

where D^{DRIFT} is an estimate of roof displacement which is 'back-calculated' from the probabilistic drift performance criterion. (Other alternatives for calculating the base shear are discussed in Collins[12] and Collins *et al.*[13]).

10. Distribute the base shear over the height of the structure in accordance with the code-specified force distribution, $\{f\}$. Determine preliminary sizes of all members and structural elements.
11. Perform a linear elastic static analysis of the structure using the code-specified force distribution, and record the lateral deflection profile $\{u_{\text{static}}\}$ once the full load is applied. Create a plot of base shear versus roof displacement from the results. Normalize $\{u_{\text{static}}\}$ by dividing each component by $(u_{\text{static}})_{\text{roof}}$. The resulting normalized deflection profile is the value of $\{\Psi_1\}$ to be used to verify the design. From the plot of base shear versus roof displacement, determine the initial slope. This slope is the current value of the global stiffness, K.
12. Recalculate L^*, M^*, P^*, and β_{LG} using the deflection profile $\{\Psi_1\}$ from Step 11. Calculate the natural frequency of the equivalent system model, ω^*, and the corresponding natural period, T^*, using

$$\omega^* = \sqrt{\frac{K\{\Psi_2\}^{\text{T}}\{f\}}{M^*}} \tag{28}$$

$$T^* = \frac{2\pi}{\omega^*} \tag{29}$$

13. If the lateral force distribution, $\{f\}$, is a function of T^*, then repeat Steps 11 and 12 until convergence in $\{\Psi_1\}$ and T^* is achieved. Otherwise, continue to Step 14.
14. Use the uniform hazard spectrum curves for displacement at period T^* (from Step 12) and determine the value of spectral displacement $S_d(T^*)$ corresponding to the target exceedance probability, p_t. Update the design base shear using equation (27). If

$$S_d(T^*) \leqslant \frac{H\Delta^{\text{S}}_{\text{CODE}}}{n\Omega_t FP^* \beta_{\text{LG}}} \tag{30}$$

then repeat the static push-over analysis performed in Step 11. If the push-over analysis predicts that the structure remains elastic when subjected to the updated design base shear, then the structural design satisfies the performance criterion for drift. (Of course, the code-specified load combinations must be checked as necessary.) If equation (30) is not satisfied, then the structure must be stiffened. If equation (30) is satisfied but the structure does not remain elastic when subjected to the maximum base shear force, then the structure must be strengthened. Repeat Steps 11–13 above as necessary.

Design and analysis procedure for the ultimate limit state

For the ultimate limit state, the structural design which satisfies the serviceability criterion is checked to ensure that the structure has adequate strength and stiffness to limit the non-linear inelastic behaviour which is expected to occur during a large earthquake. Given threshold values of interstorey drift ratio ($\Delta^{\text{U}}_{\text{CODE}}$) and global ductility ($\mu_{\text{CODE}}$) for the ultimate limit state and a target exceedance probability (p_t), the performance criteria for drift and ductility are as given in equations (17) and (19). For convenience and simplicity, the value of p_t is assumed to be the same in both equations. The steps for this level of design are outlined below.

1. Develop a structural model which can be used in a *non-linear inelastic* static push-over analysis. The model should use *best-estimate* values of material yield strengths instead of nominal values.
2. Perform an incremental non-linear push-over analysis of the structure using the prescribed lateral force distribution, $\{f\}$, scaled incrementally by a factor V. Since this is a non-linear analysis, all gravity loads that would be considered in the code-specified load combinations should be applied to the

structure before applying the lateral loads. Generate a plot of the scale factor, V, versus the top (roof) displacement of the structure, D. Continue to increase the loading until the top storey displacement is well beyond $\Delta_{target}H$ where H is the total height of the structure and Δ_{target} is a code-prescribed global drift ratio. The appropriate value of Δ_{target} may be dependent on the type of structural framing system, and it must be large enough so that the structure indeed yields and the slope of the V–D diagram begins to deviate from the initial slope. Record the lateral deflection profile, $\{u_{static}\}$, of the structure when $D = D_{target} = \Delta_{target}H$. Normalize $\{u_{static}\}$ by dividing each element by $(u_{static})_{roof}$. The resulting normalized lateral deflection profile is $\{\Psi_1\}$.

3. Approximate the multi-linear V–D diagram generated in Step 2 by a bilinear V–D curve. The initial slope (K) of the bilinear curve should be equal to the initial slope of the actual curve. The second slope and the global yield point (D_y) can be estimated by equating the areas under the diagrams or by simply extrapolating the slope of the actual curve (at $D = D_{target}$) backwards. Also, determine the ratio of the second slope to the first slope, α, for the approximate bilinear diagram.
4. Calculate M^*, L^*, P^*, ω^*, T^*, and β_{LG} using the deflection profile $\{\Psi_1\}$ obtained from Step 2. (See equations (21)–(24), (28) and (29).)
5. Determine Ω_t^{μ} and n_U^{DISP}, and calculate the target ductility, μ_t, using equation (18).
6. For the set of parameters (μ_t, p_t, T^*, α), find the value of the required yield force coefficient, $C_y(\mu = \mu_t)$, from the uniform hazard spectra.
7. Calculate the required global yield displacement, D_y^t, using

$$D_y^t = \Omega_t^F P^* F g \left(\frac{T^*}{2\pi}\right)^2 C_y(\mu_t) \tag{31}$$

where Ω_t^F is the appropriate value of the design factor for the target probability, target ductility, and period of the equivalent system model.

8. If the global yield displacement of the structure, D_y, is *larger* than the required yield displacement obtained using equation (31), then the structure satisfies the global ductility performance criterion. If D_y is *smaller* than the required yield displacement, then the structure must be strengthened (and possibly stiffened).
9. If D_y is significantly larger than the required value, then determine the ductility value $\mu'(\mu' \leqslant \mu_t)$ corresponding to D_y such that the probability of exceeding μ' (for the equivalent system model) is equal to p_t. (This will require interpolation between uniform hazard curves.) The yield force coefficient corresponding to μ' can be obtained from

$$C_y(\mu') = \frac{D_y}{\Omega_t^F P^* F g \left(\frac{T^*}{2\pi}\right)^2} \tag{32}$$

(If Ω_t^F is a strong function of ductility, then determining μ' will require iteration.)

10. Determine the values of Ω_t^{Δ} and n_U^{DRIFT}. If

$$\Delta_{CODE}^U \geqslant \mu' \frac{\beta_{LG}}{H} \Omega_t^{\Delta} n_U^{DRIFT} D_y \tag{33}$$

then the structure satisfies the performance criterion for interstorey drift ratio. If equation (33) is not satisfied, then the structure must be stiffened (and possibly strengthened).

Design examples: two-storey moment-resisting steel frame

To demonstrate the use of the proposed design and analysis procedure, two examples related to the design of a two-storey moment resisting steel frame are presented. These two examples clearly demonstrate the importance of considering strength and stiffness simultaneously when designing structures to satisfy displacement-based performance criteria.

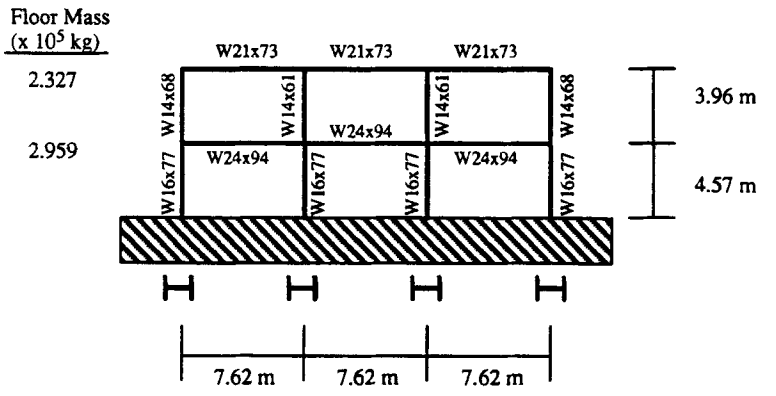

$T_{BARE\ FRAME}$ = 0.91 second

Parameters for equivalent system – linear elastic analysis

$\{\Psi_1\}^T$ (top to bottom) = {1.00, 0.532} K = 1.82 x 10^7 N/m

Parameters for equivalent system – nonlinear inelastic analysis

$\{\Psi_1\}^T$ (top to bottom) = {1.00, 0.615} K = 1.80 x 10^7 N/m

D_y = 6.6 cm α (strain hardening) = 10%

Figure 11. Information related to the linear and non-linear static push-over analyses of the two-storey MRF (original design)

In the first example, a two-storey moment frame designed in accordance with the 1991 Uniform Building Code[43] is considered. The general layout of the frame and other pertinent information is shown in Figure 11. The purpose of this example is to determine the values of Δ^S_{CODE} and Δ^U_{CODE} required for the design to satisfy the drift performance criteria presented in equations (14) and (19) *if* the target exceedance probability, p_t, is equal to 50 per cent in 50 yr for the serviceability limit state and 10 per cent in 250 yr for the ultimate limit state. The detailed calculations are provided in Collins[12] and Collins *et al.*[13] For the chosen target probabilities, the values of Δ^S_{CODE} and Δ^U_{CODE} must be greater than 0·0060 (0·6 per cent) and 0·025 (2·5 per cent), respectively, for this design to be acceptable.

In the second example, *hypothetical* performance criteria are defined, and a modified two-storey moment frame design is developed. Pertinent information on the modified design is shown in Figure 12. The hypothetical performance criteria are as follows:

serviceability limit state

$$p_t = 50 \text{ per cent in } 50 \text{ yr}$$

$$\Delta^S_{CODE} = 0{\cdot}5 \text{ per cent}$$

ultimate limit state

$$p_t = 10 \text{ per cent in } 250 \text{ yr}$$

$$\Delta^U_{CODE} = 1{\cdot}5 \text{ per cent}$$

$$\mu_{CODE} = 4$$

The values of Δ^S_{CODE} and Δ^U_{CODE} are consistent with the values identified by Foutch *et al.*[48] as being representative of the drift ratios corresponding to the onset of non-structural damage and life-threatening conditions, respectively. The chosen combinations of drift thresholds, target global ductility, and target

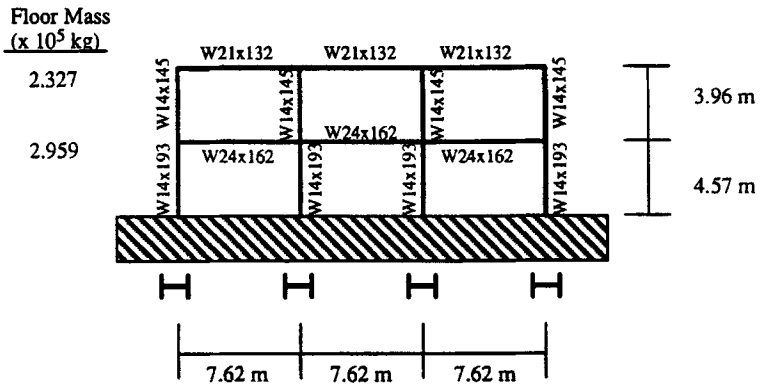

$T_{BARE\ FRAME}$ = 0.62 second

Parameters for equivalent system (revised design) – linear elastic analysis

$\{\Psi_1\}^T$ (top to bottom) = {1.00, 0.560} $K = 4.06 \times 10^7$ N/m

Parameters for equivalent system (revised design) – nonlinear inelastic analysis

$\{\Psi_1\}^T$ (top to bottom) = {1.00, 0.627} $K = 4.05 \times 10^7$ N/m

D_y = 7.1 cm α (strain hardening) = 10%

Figure 12. Information on the two-storey MRF redesigned for hypothetical performance criteria

exceedance probabilities are arbitrary and are used here for demonstration purposes only. These hypothetical performance criteria may or may not be appropriate for use in code specifications for this type of structure. They are used merely to demonstrate how the proposed design and analysis procedure can be used. The calculations for this example are summarized in Appendix II to this paper.

The two-storey moment frame shown in Figure 11 was used as the starting point for developing the modified design. Using the proposed dual-level design procedure, several intermediate designs were evaluated and updated before arriving at the modified design shown in Figure 12. The drift performance criterion for the ultimate limit state proved to be the controlling criterion in this example; the criterion for global ductility was easily satisfied. The global stiffness, K, of the modified design is about 2.2 times the global stiffness of the two-storey frame considered in the first example. The base shear strength of the modified design is also higher by about the same factor; thus, the global yield displacements of the two designs are comparable. The total weight of all structural members in the modified design is about 183 kN (41·2 kips), and the total weight of the members in the original design is about 91·2 kN (20·5 kips). However, a comparison of the total weights of the members may be somewhat misleading since no attempt was made to select 'optimum' (i.e., minimum weight) members for the modified design.

SUMMARY AND CONCLUSIONS

This paper describes a reliability-based seismic design procedure for building structures. The key features of the proposed procedure include the following: (1) Two levels of design corresponding to two structural limit states are used. The first level of design corresponds to a serviceability limit state, and the performance objective is to ensure elastic (or nearly elastic) response of the structure during small to moderate earthquakes. The second level of design corresponds to an ultimate limit state, and the performance objective is to

control the non-linear inelastic behaviour which is expected to occur during severe earthquakes. (2) Uniform hazard spectra for both linear elastic and non-linear inelastic response are used to provide probabilistic information on seismic demand. The probabilities associated with the spectra reflect the likelihood of earthquake occurrences as well as the severity of the earthquake ground motion when an earthquake does occur. (3) SDOF models are used to evaluate the performance of the structure in terms of the probability of exceeding displacement-based limit state criteria. (4) Linear and non-linear static push-over analyses are used to obtain global response characteristics of the structure. The results of the push-over analyses are used to calibrate the parameters of the SDOF models of the structure. (5) A recently proposed methodology for quantifying site soil effects is incorporated into the procedure. This methodology uses information on the structural period and the mean shear wave velocity of the foundation soils. (6) Deterministic design-checking equations are used to determine compliance with code requirements for global ductility and interstorey drift. These equations incorporate design factors (analogous to load and resistance factors) which account for the uncertainty in estimating site soil effects, the approximate nature of the SDOF analysis models, and the uncertainty in the seismic hazard.

The proposed reliability-based procedure is different from current procedures in four significant ways. First, non-linear behaviour is treated explicitly (albeit approximately) using information from static push-over analyses. Such analyses should help designers to better appreciate the non-linear behaviour which is expected to occur during large earthquakes and to identify critical regions of the structure requiring careful detailing and design. Second, the procedure explicitly accounts for the approximate nature of the simple analysis models, the uncertainty in the local seismic hazard, and the uncertainty in the methods used to estimate the effects of site soils. Such uncertainties and approximations must be accounted for in a rational manner to achieve reliable structural designs. Third, since it is difficult to achieve multiple performance objectives using a single design earthquake, two levels of ground motion are considered. Fourth, the procedure is a true performance-based procedure in the sense that explicit probabilistic criteria are specified for structural response (i.e. performance).

Before the proposed procedure is implemented in future seismic design codes, there are several issues which must be addressed. First, the procedure has been developed primarily for steel building structures. Additional research is needed to extend the procedure to structures constructed of reinforced concrete, masonry, etc. Second, probabilistic performance criteria must be established for various building materials and framing systems. This requires decisions on the target probabilities of exceedance for each limit state and the target values of interstorey drift ratio, global ductility, and possibly other measures of structural performance. Third, additional research is needed to develop techniques to account for the influence of non-structural components on the dynamic properties and response behaviour of building structures. Fourth, additional studies are needed to evaluate whether or not the equivalent system methodology is 'robust'. Fifth, additional studies are needed to evaluate the sensitivity of the design factors to site-specific seismic hazard. Finally, the design equations and design factors should be modified or generalized to explicitly include the uncertainty in estimating the capacity of the structure.

ACKNOWLEDGEMENTS

Financial support for this research has been provided by the National Science Foundation (US) through grants NSF BCS-9106390 and NSF NCEER 93-4102B. This support is gratefully acknowledged. The conclusions and opinions expressed in this paper are those of the authors and do not necessarily represent the views of the sponsor. Computer support, equipment, and facilities were provided by the University of Illinois. The authors would like to thank Dr. S. Schneider, Dr. S. Wood, Dr. T. Saito, Dr. S.W. Han, K. Elwood, and two anonymous reviewers for their helpful comments and suggestions.

APPENDIX I

This appendix presents some of the formulae needed to apply the equivalent system methodology. In these formulas, the vector $\{f\}$ is a normalized lateral force vector used in the static push-over analysis. The vector is

normalized such that the corresponding base shear is equal to 1. The quantity K is the global stiffness ($= V/D$) determined from the initial portion of the plot of base shear (V) versus roof displacement (D).

$$M^* = \{\Psi_2\}^T[M]\{\Psi_1\}, \qquad C^* = \{\Psi_2\}^T[C]\{\Psi_1\}, \qquad K^* = K\{\Psi_2\}^T\{f\}$$

$$\omega^* = \sqrt{K^*/M^*}, \qquad P^* = \{\Psi_2\}^T[M]\{1\}/M^*, \qquad C^*/M^* = 2\zeta\omega^*$$

APPENDIX II

This appendix outlines some of the calculations required to show that the two-storey moment-resisting frame shown in Figure 12 satisfies the following hypothetical performance criteria:

serviceability limit state

$$p_t = 50 \text{ per cent in } 50 \text{ yr}$$

$$\Delta^S_{CODE} = 0{\cdot}5 \text{ per cent}$$

ultimate limit state

$$p_t = 10 \text{ per cent in } 250 \text{ yr}$$

$$\Delta^U_{CODE} = 1{\cdot}5 \text{ per cent}$$

$$\mu_{CODE} = 4$$

Calculations for the serviceability limit state

Total structure height $H = 8{\cdot}53$ m (28 ft). The height of the first storey (h_1) is 4·57 m (15 ft), and the height of the second storey (h_2) is 3·96 m (13 ft). From a linear elastic push-over analysis, $K = 4{\cdot}06 \times 10^7$ N/m and $\{\Psi_1\}^T = \{1{\cdot}00, 0{\cdot}560\}$. All equivalent system parameters are calculated using the base shear formulation (i.e. $\{\Psi_2\}^T = \{1{\cdot}0, 1{\cdot}0\}$).

$$M^* = \{\Psi_2\}^T[M]\{\Psi_1\} = \{1{\cdot}0, 1{\cdot}0\}\begin{bmatrix} 2{\cdot}327 & 0 \\ 0 & 2{\cdot}959 \end{bmatrix}\begin{Bmatrix} 1{\cdot}00 \\ 0{\cdot}560 \end{Bmatrix}(\times 10^5 \text{ kg}) = 3{\cdot}98 \times 10^5 \text{ kg}$$

$$L^* = \{\Psi_2\}^T[M]\{1\} = \{1{\cdot}0, 1{\cdot}0\}\begin{bmatrix} 2{\cdot}327 & 0 \\ 0 & 2{\cdot}959 \end{bmatrix}\begin{Bmatrix} 1{\cdot}0 \\ 1{\cdot}0 \end{Bmatrix}(\times 10^5 \text{ kg}) = 5{\cdot}29 \times 10^5 \text{ kg}$$

$$P^* = L^*/M^* = 1{\cdot}33$$

$$\beta_{LG} = H\left[\frac{\Psi_{1,i} - \Psi_{1,i-1}}{h_i}\right]_{max} = \max\left\{\frac{1{\cdot}0 - 0{\cdot}560}{396 \text{ cm}}, \frac{0{\cdot}560 - 0}{457 \text{ cm}}\right\}(853 \text{ cm}) = 1{\cdot}05$$

$$K^* = K, \qquad \omega^* = \sqrt{K^*/M^*} = 10{\cdot}1 \text{ rad/s}. \qquad T^* = 2\pi/\omega^* = 0{\cdot}62 \text{ s}$$

By linearly interpolating between points on the uniform hazard curve (elastic response) for a probability $p_t = 50$ per cent in 50 yr, $C_e(T = T^*) = 0{\cdot}37$. The corresponding value of $S_d(T^*)$ is

$$S_d(T^*) = C_e(T^*)\left[g\left(\frac{T^*}{2\pi}\right)^2\right] = (0{\cdot}37)\left[981\,\frac{\text{cm}}{s^2}\left(\frac{0{\cdot}62 \text{ s}}{2\pi}\right)^2\right] = 3{\cdot}5 \text{ cm}$$

From Table VI, using linear interpolation, $\Omega_t(T^*) = 1{\cdot}21$. The value of n is assumed to be 1·0. The soil factor, F, is calculated assuming $v_{ref} = 540$ m/s, $v_{site} = 1335$ m/s, and $m = 0{\cdot}65$. Thus,

$$F = \left(\frac{v_{ref}}{v_{site}}\right)^m = \left(\frac{540}{1335}\right)^{0{\cdot}65} = 0{\cdot}56$$

The design requirement is

$$S_d(T^*) \leqslant \frac{H\Delta^{S}_{CODE}}{\Omega_t F n P^* \beta_{LG}}$$

$$\leqslant \frac{(853\text{ cm})(0{\cdot}005)}{(1{\cdot}21)(0{\cdot}56)(1{\cdot}0)(1{\cdot}33)(1{\cdot}05)}$$

$$\leqslant 4{\cdot}5\text{ cm}$$

Since $S_d(T^*) = 3{\cdot}5$ cm is less than 4·5 cm, the drift performance criterion for the serviceability limit state is satisfied.

Calculations for the ultimate limit state

From the nonlinear push-over analysis, $K = 4{\cdot}05 \times 10^7$ N/m, $D_y = 7{\cdot}1$ cm, $\{\Psi_1\}^T = \{1{\cdot}00, 0{\cdot}627\}$, and $\alpha = 10$ per cent. (Note: The uniform hazard curves for non-linear response presented earlier are based on $\alpha = 5$ per cent. For demonstration purposes, it is assumed that the effects of different values of α are negligible, and the curves for $\alpha = 5$ per cent are used without modification.)

$$M^* = 4{\cdot}18 \times 10^5\text{ kg}, \quad L^* = 5{\cdot}29 \times 10^5\text{ kg}, \quad P^* = 1{\cdot}27, \quad \beta_{LG} = 1{\cdot}17; \quad K^* = K, \quad \omega^* = 9{\cdot}8\text{ rad/s},$$

$$T^* = 0{\cdot}64\text{ s}$$

The values of n_U^{DISP} and n_U^{DRIFT} are assumed to be the same as those for the two-storey MRF listed in Tables III and IV. Thus, $n_U^{DISP} = 0{\cdot}89$ and $n_U^{DRIFT} = 0{\cdot}96$. Both Ω_t^{μ} and Ω_t^{Δ} are assumed to be 1·1.

The target ductility is

$$\mu_t = \frac{\mu_{CODE}}{\Omega_t^{\mu} n_U^{DISP}} = \frac{4}{(1{\cdot}1)(0{\cdot}89)} = 4{\cdot}1 \quad (use\ 4{\cdot}0)$$

Interpolating between ordinates on the uniform hazard curve (non-linear response) for $p_t = 10$ per cent in 250 yr, $C_y(\mu_t, T^*) = 0{\cdot}29$. The soil factor is 0·56 as before. From Table VII, $\Omega_t^F(\mu_t, T^*) = 1{\cdot}27$. The required global yield displacement is

$$D_y^t = \Omega_t^F P^* F g \left(\frac{T^*}{2\pi}\right)^2 C_y(\mu, T^*) = (1{\cdot}27)(1{\cdot}27)(0{\cdot}56)(981\text{ cm/s}^2)\left(\frac{0{\cdot}64\text{ s}}{2\pi}\right)^2 (0{\cdot}29) = 2{\cdot}7\text{ cm}$$

Since the actual global yield displacement, D_y, is greater than 2·7 cm, the design satisfies the performance criterion for global ductility. Since D_y is much larger than 2·7 cm, it is necessary to find the ductility μ' corresponding to D_y and p_t. The yield force coefficient corresponding to D_y is

$$C_y(\mu', T^*) = \frac{D_y}{\Omega_t^F P^* F g (T^*/2\pi)^2} = \frac{7{\cdot}1\text{ cm}}{(1{\cdot}27)(1{\cdot}27)(0{\cdot}56)(981\text{ cm/s}^2)(0{\cdot}64\text{ s}/2\pi)^2} = 0{\cdot}77$$

Using linear interpolation between the uniform hazard curve for elastic response [which can be interpreted as $C_y(\mu = 1)$] and the curve for $C_y(\mu = 2)$, the value of μ' corresponding to $C_y(\mu = \mu')$ is approximately 1·5.

The requirement for interstorey drift ratio is

$$\Delta^{U}_{CODE} \geqslant \mu' \frac{\beta_{LG}}{H} \Omega_t^{\Delta} n_U^{DRIFT} D_y$$

$$\geqslant (1{\cdot}5)\frac{1{\cdot}17}{853\text{ cm}}(1{\cdot}1)(0{\cdot}96)(7{\cdot}1\text{ cm})$$

$$\geqslant 0{\cdot}0154$$

Although $\Delta^{U}_{CODE} = 0{\cdot}015$ is not larger than 0·0154, the discrepancy is judged to be negligible. Thus, the performance criterion for interstorey drift is satisfied.

REFERENCES

1. G. V. Berg, *Elements of Structural Dynamics*, Prentice-Hall, Englewood Cliffs, NJ, 1989.
2. Applied Technology Council (ATC-34), *A Critical Review of Current Approaches to Earthquake-Resistant Design*, Final Draft, 1994.
3. Y. K. Wen, 'Reliability-based design under multiple loads', *Struct. safety* **13**, 3–19 (1993).
4. Y. K. Wen, 'Building reliability and code calibration', *Earthquake spectra* **11**, 269–296 (1995).
5. V. V. Bertero, J. C. Anderson, H. Krawinkler, E. Miranda and CUREe/Kajima Research Teams, 'Design guidelines for ductility and drift limits: review of state-of-the-practice and state-of-the-art in ductility and drift-based earthquake-resistant design of buildings', *EERC Report UCB/EERC-91/15*, Earthquake Engineering Research Center, University of California, Berkeley, CA, 1991.
6. R. D. Bertero and V. V. Bertero, 'Tall reinforced concrete buildings: conceptual earthquake-resistant design methodology', *EERC Report No. UCB/EERC-92/16*, Earthquake Engineering Research Center, University of California, Berkeley, CA, 1992.
7. J. D. Osteraas and H. Krawinkler, 'Strength and ductility considerations in seismic design', *Report No.* 90, John A. Blume Earthquake Engineering Center, Stanford University, CA, 1990.
8. R. D. Borcherdt, 'New developments in estimating site effects on ground motion', in *Proc. seminar on new developments in earthquake ground motion estimation and implications for engineering design practice*, Applied Technology Council, ATC 35-1, 1994.
9. R. D. Borcherdt, 'Estimates of site-dependent response spectra for design (methodology and justification)', *Earthquake spectra* **10**, 617–653 (1994).
10. R. K. McGuire, 'Seismic structural response risk analysis, incorporating peak response regressions on earthquake magnitude and distance', *Report R74-51, Structures Publication No. 399*, Department of Civil Engineering, Massachusetts Institute of Technology, MA, 1974.
11. R. T. Sewell and C. A. Cornell, 'Seismic hazard analysis based on limit state structural damage', in *Proc. 5th International conf. on applications of statistics and probability in soil and structural engineering*, University of British Columbia (Canada), 1987, pp. 1020–1026.
12. K. R. Collins, 'Investigation of alternative seismic design procedures for standard buildings', *Ph.D. Thesis*, Department of Civil Engineering, University of Illinois at Urbana-Champaign, IL, 1995.
13. K. R. Collins, Y. K. Wen and D. A. Foutch, 'Investigation of alternative seismic design procedures for standard buildings', *Structural Research Series No. 600*, Department of Civil Engineering, University of Illinois at Urbana-Champaign, IL, 1995.
14. S. T. Algermissen, D. M. Perkins, P. C. Thenhaus, S. L. Hanson and B. L. Bender, 'Probabilistic estimates of maximum acceleration and velocity in rock in the contiguous united states', *Open File Report 82-1033*, United States Department of the Interior, Geological Survey, 1982.
15. S. T. Algermissen, D. M. Perkins, P. C. Thenhaus, S. L. Hanson, and B. L. Bender, 'Probabilistic earthquake acceleration and velocity maps for the United States and Puerto Rico', *USGS Miscellaneous Field Studies Map MF-2120* (2 sheets), United States Department of the Interior, Geological Survey, 1990.
16. S. T. Algermissen, E. V. Leyendecker, G. A. Bollinger, N. C. Donovan, J. E. Ebel, W. B. Joyner, R. W. Luft and J. P. Singh, 'Probabilistic ground-motion hazard maps of response spectral ordinates for the United States', in *Proc. 4th int. conf. on seismic zonation*, Stanford University, Stanford, CA, 1991, pp. 687–694.
17. S. T. Algermissen and E. V. Leyendecker, 'Technique for uniform hazard spectra estimation in the US', *Proc. of the 10th world conf. on earthquake engineering*, Madrid, Spain, Balkema, Rotterdam, 1992, pp. 391–397.
18. Building Seismic Safety Council (BSSC), *NEHRP Recommended Provisions for the Development of Seismic Regulations for New Buildings*, Vols 1 and 2, prepared for and issued by the Federal Emergency Management Agency (FEMA), 1992.
19. C. A. Cornell and S. R. Winterstein, 'Temporal and magnitude dependence in earthquake recurrence models', *Lecture Notes in Engineering, Stochastic Approaches in Earthquake Engineering*, Springer, Berlin, 1987.
20. United States Department of the Interior, Geological Survey (USGS), 'Probabilities of large earthquakes occurring in California on the San Andreas Fault', *USGS Open File Report 88-398*, 1988.
21. M. I. Todorovska, 'Comparison of response spectrum amplitudes from earthquakes with a lognormally and exponentially distributed return period', *Soil dyn. earthquake eng.* **13**, 97–116 (1994).
22. D. M. Boore, W. B. Joyner and T. E. Fumal, 'Estimation of response spectra and peak accelerations from western North American earthquakes: an interim report', *Open File Report 93-509*, US Geological Survey, 1993.
23. D. M. Boore, W. B. Joyner and T. E. Fumal, 'Estimation of response spectra and peak accelerations from western North American earthquakes: an interim report—Part 2', *Open File Report 94-127*, US Geological Survey, 1994.
24. B. K. Bender and D. M. Perkins, 'Treatment of parameter uncertainty and variability for a single seismic hazard map', *Earthquake spectra* **9**, 165–195 (1993).
25. P. G. Somerville, N. F. Smith, R. W. Graves and N. Abrahamson, 'Accounting for near-fault rupture directivity effects in the development of design ground motions', (draft) *ASME/JSME PVP Conf.*, 1995.
26. R. W. Clough and J. Penzien, *Dynamics of Structures*, McGraw-Hill, New York, 1975.
27. M. D. Trifunac, 'Long period Fourier amplitude spectra of strong motion acceleration', *Soil dyn. earthquake eng.* **12**, 363–382 (1993).
28. B. A. Bolt, 'Seismicity: assessment of seismic intensity', *Seminar Notes, Advances in Earthquake Engineering Practice*, University of California, Berkeley, CA, 31 May–4 June, 1994.
29. A. Frankel, P. Thenhaus, D. Perkins and E. V. Leyendecker, 'Ground motion mapping—past, present and future', in *Proc. seminar on new developments in earthquake ground motion estimation and implications for engineering design practice*, Applied Technology Council, ATC 35-1, 1994.
30. C. H. Yeh and Y. K. Wen, 'Modeling of nonstationary earthquake ground motion and biaxial and torsional response of inelastic structures', *Structural Research Series Report No. 546*, Department of Civil Engineering, University of Illinois at Urbana-Champaign, IL, 1989.
31. R. V. Whitman (ed.), 'Workshop on ground motion parameters for seismic hazard mapping,' *NCEER-89-0038*, 1989.
32. E. Miranda and V. V. Bertero, 'Evaluation of strength reduction factors for earthquake-resistant design', *Earthquake spectra* **10**, 357–379 (1994).
33. A. A. Nassar and H. Krawinkler, 'Seismic demands for SDOF and MDOF systems', *Report No. 95*, John A. Blume Earthquake Engineering Center, Stanford University, CA, 1991.

34. Working Group on California Earthquake Probabilities, 'Seismic hazards in southern California: probable earthquakes, 1994 to 2024', *Bull. seism. soc. Am.* **85**, 379–439 (1995).
35. M. Saiidi and M. Sozen, 'Simple and complex models for nonlinear seismic response of reinforced concrete structures', *Structural Research Series Report No.* 465, Department of Civil Engineering, University of Illinois at Urbana-Champaign, IL, 1979.
36. S. A. Mahin and J. Lin, 'Construction of inelastic response spectra for single-degree-of-freedom systems: computer program and applications', *EERC Report No. UCB/EERC-83/17*, Earthquake Engineering Research Center, University of California, Berkeley, CA, 1983.
37. X. Qi and J. P. Moehle, 'Displacement design approach for reinforced concrete structures subjected to earthquakes', *EERC Report No. UCB/EERC-91/02*, Earthquake Engineering Research Center, University of California, Berkeley, CA, 1991.
38. J. M. Biggs, *Introduction to Structural Dynamics*, McGraw-Hill, New York, 1964.
39. J. C. Anderson, 'Dynamic response of buildings', in F. Naeim (ed.), *The Seismic Design Handbook*, Van Nostrand Reinhold, New York, 1989.
40. J. F. Bonacci, 'Design forces for drift and damage control: a second look at the substitute structure approach', *Earthquake spectra* **10**, 319–331 (1994).
41. P. Fajfar and M. Fischinger, 'N2—a method for non-linear seismic analysis of regular buildings', *Proc. 9th world conf. on earthquake eng.* **V**, 111–116 (1988).
42. E. Miranda, 'Seismic evaluation and upgrading of existing buildings', *Ph.D. Thesis*, Department of Civil Engineering, University of California, Berkeley, CA, 1991.
43. International Conference of Building Officials (ICBO), *Uniform Building Code*, Whittier, California, 1991.
44. Y. K. Wen, H. Hwang and M. Shinozuka, 'Development of reliability-based design criteria for buildings under seismic load', *NCEER-94-0023*, National Center for Earthquake Engineering Research, 1994.
45. United States Department of Energy (USDOE), 'Natural phenomena hazards design and evaluation criteria for department of energy facilities', *DOE Standard DOE-STD-1020-94*, 1994.
46. American Institute of Steel Construction (AISC), *AISC Manual of Steel Construction—Load & Resistance Factor Design*, 1st edn., AISC, Chicago, IL, U.S.A., 1986.
47. H. Hwang, B. Ellingwood, M. Shinozuka and M. Reich, 'Probability-based design criteria for nuclear plant structures', *J. struct. eng. ASCE* **113**, 925–942 (1987).
48. D. A. Foutch, C.-Y. Yu and Y. K. Wen, 'Reliability of steel frame buildings under seismic load', *Proc. 10th world conf. on earthquake eng.* Madrid, Spain, Balkema, Rotterdam, (1992) pp. 4423–4427.